MEASUREMENT AND RENDERING OF AUTOMOTIVE COATINGS WITH A NOVEL TEXTURE CAMERA

BY JAYANT SILVA

A thesis submitted to the

Graduate School—New Brunswick

Rutgers, The State University of New Jersey

in partial fulfillment of the requirements

for the degree of

Master of Science

Graduate Program in Electrical and Computer Engineering

Written under the direction of

Dr. Kristin J. Dana

and approved by

_____

_____

_____

New Brunswick, New Jersey

October, 2010

ABSTRACT OF THE THESIS

Measurement and Rendering of Automotive Coatings with a Novel Texture Camera

by Jayant Silva

Thesis Director: Dr. Kristin J. Dana

In an effort to create more dynamic looking automobiles, there is an ever increasing trend among automobile manufacturers towards the use of metallic coatings in the finish of a vehicle. These coatings consist of transparent colorants mixed with metallic flakes. The flakes in the coating cause a change in color and brightness of the finish with viewing and illumination direction. This change in appearance accentuates the curves of a car, making it visually more attractive. Besides this angular dependence on viewing/illumination direction, the metallic finishes also exhibit a visually complex texture. Depending on the properties of the finish and the viewing and illumination conditions, the flakes exhibit a sparkle like texture, while the glossy clear coat may show a rough or smooth surface. As a result of these complex visual attributes, capturing the appearance and finding a perfect color match for a metallic finish is a non trivial task.

Traditional methods of visual color evaluation and five angle color measurement can neither sufficiently capture nor characterize the angular and spatial variation in appearance of a metallic coating. Instead, we use the BTF (bidirectional texture function) to capture the variation in appearance of the coating with illumination and viewing

direction. We use a novel texture camera to simultaneously capture the BRDF (bidirectional reflectance distribution function) and BTF of the coatings. We use the unique BRDF of each finish to develop a completely objective and automated match measure that shows a high correlation with the visual judgement of color matching experts. We then use the measured BTFs along with a novel texture synthesis technique to create photorealistic renderings of the coatings that reproduces all the visual effects of these complex coatings. We also present a novel material recognition method using the Texcam images.

Acknowledgements

I would like to thank my advisor Dr. Kristin Dana for her guidance and support throughout my graduate research work at Rutgers. Her patience and advice during our numerous discussions have helped shape my thinking and the way I conduct my research. I also gratefully acknowledge the institutional support that I have received while working on this project from PPG through their grant. I would especially like to thank Gregory McCollum for his constant support during this project, and for making available to us the data and paint panels used throughout this work. During my time at Rutgers, I have had the good fortune of sharing my lab with Siddharth Madan, Wenjia Yuan and Rahul Sheth. Interacting with them has been a wonderful experience. I thank Siddharth for being there to answer my many questions and Rahul for his work on the Texcam.

Table of Contents

List of Figures

Chapter 1

Introduction

Most real world surfaces show a variation in appearance with viewing and illumination direction. Besides an angular dependency, they also show a spatial variation in color i.e. they exhibit some sort of texture. Among the surfaces we commonly encounter, metallic paint produces several complex visual effects like a change in color and brightness with viewing and illumination angle, a sparkle like texture as well as specular reflections. These effects make it difficult to accurately measure and model metallic coatings. Because of their widespread use in the automobile industry there is significant interest in their imaging and analysis. In particular a solution is needed to the problem of finding a completely automated and objective color match for a metallic coating, which agrees with the visual evaluation of color matching experts.

Finding a color match that agrees with the visual judgement involves understanding the visually important attributes of a metallic coating. Metallic coatings show a large change in brightness and color with small change in viewing and illumination angle. In bright sunlight, it appears to sparkle besides showing a bright specular reflection from the gloss. The surface of the coating can also have an orange peel like texture which influences its perception. Capturing all these visual attributes of the coating is the key to its analysis and modeling. In this thesis we first develop an understanding of the visually important attributes of a metallic and present a method to accurately capture these effects using a novel imaging device - the texture camera (Texcam).

The next contribution of this thesis is to develop a completely automated and objective match measure for the metallic coatings which shows a high correlation with the visual judgement of color matching experts. The match measure is based on the measured reflectance of the coatings. The Texcam is able to simultaneously capture a

surface's bidirectional reflectance distribution function (BRDF) as well as its bidirectional texture function (BTF) by measuring its reflectance over a continuum of viewing and illumination angles. The BRDF of the coating as imaged by the Texcam is used to characterize its change in brightness and color with viewing and illumination angle. The BTF of the coating is used to analyze the its visual attributes such as the sparkle, gloss and orange peel.

Finally, the ability of the Texcam to accurately capture the appearance of a metallic coatings and all its complex visual attributes makes it especially useful in the photo-realistic rendering of the coating. The BTF of the coating can be used in image based rendering to produce virtual samples of the coating where the customer would like to preview what a particular coating looks like. The BTF of the coating as imaged by the Texcam consists of small images of the sample surface over multiple viewing and illumination directions. In order to cover a larger surface area, like a virtual paint panel, we need to synthesize larger images from the small input BTFs. The use of traditional texture synthesis techniques for a high dimensional input texture such as a BTF produces unwanted artifacts besides taking a large amount of time for execution. The second contribution of this thesis is to introduce a novel texture synthesis technique that not only removes these artifacts but also greatly reduces the amount of time required for execution. We then use these synthesized images to create photo-realistic virtual samples of a metallic coating that shows all of its visually important attributes.

The remainder of this thesis is divided into three additional chapters. Chapter two offers a discussion on the composition and visual attributes of metallic coatings as well as currently used matching techniques. In chapter three we discuss their measurement using the Texcam and use these measurements to develop a match measure for the coatings. Chapter four deals with the texture synthesis and photorealistic rendering of the metallic coatings. Finally, there is also an appendix which includes important information about the proper setup and operation of the Texcam.

Chapter 2

Automobile Paints

Figure 2.1: Appearance of an automotive coating. Metallic flakes present within the coating cause the blue finish of this car to show a change in brightness with viewing angle. The change in brightness enhances the visual appearance of the curved body of the car. The sparkle and texture of the finish further add to its dynamic appearance.

The exterior appearance and the finish of a car play a major role in how a customer perceives its quality. In an effort to create more dynamic looking automobiles, there is an ever increasing trend among automobile manufacturers towards the use of special effect pigments in the finish of a vehicle. Among the special effect pigments, metallic coatings represent one of the oldest and most popular effect coatings. These coatings consist of metallic flakes and colored pigment particles suspended in a binder, covered by a transparent clear coat[1][2]. Metallic effect coatings provide a broader range of appearance attributes than is available from traditional solid colors. They exhibit a

change in color and brightness with viewing and illumination direction. This change in appearance accentuates the curves of a car, making it visually more attractive. Besides this angular dependence on viewing/illumination direction, the metallic finishes also exhibit a visually complex texture. Depending on the properties of the finish and the viewing and illumination conditions, the flakes exhibit a sparkle like texture, while the glossy clear coat may show a rough or smooth surface. As a result of these complex visual attributes, imaging and color matching of a metallic finish is a non trivial task.

2.1 Composition of Metallic paints

Metallic finishes produce a number of complex visual effects. These visual effects are a result of the composition of a metallic finish and as well as the application process. The steps involved in applying a metallic finish to a car as described in [3] are as follows - the car body first undergoes pretreatment and electrocoating to protect it from corrosion, and a primer is then used for leveling the surface and providing it with chip protection. After this initial treatment, it is the function of the top coat layers to give color and durability to the coating system. The top coat is composed of a pigment with a clear coat applied over it. Pigments are used to add color to the top coat, forming a base coat. To protect the pigment from the environment, a clear coat is applied over the colored base coat. The clear coat gives the finish a luster and offers protection from sunlight, scratches and corrosion. It is worthwhile to understand the nature of each of these components and how they affect the visual appearance of the finish.

Pigments and Color

Pigments are used to bring color to the car. A pigment is any solid colored particle which is insoluble in the medium in which it is incorporated. The pigment retains its crystal or particulate structure throughout the coloration process. The appearance of the surface that is colored with the pigment particles is altered through selective absorption or scattering of light. This interaction of light with the pigment particles depends on their chemical composition and by the shape and size of the pigment particle,

which is determined by the pigment manufacturing process as well as the paint making process[3]. Aluminium effect pigments are used for metallic shades, causing a change in lightness with viewing angle, called lightness flop. Mica effect pigments are used in pearlescent shades, causing a change in color with viewing angle, called color flop. Finally, dispersants or grinding resins are used to bind the pigment surface and support the dispersion process and stabilize the final dispersion and settling of the pigment.

Basecoat and Clearcoat

The basecoat consists of the pigment particles suspended in a binder. Basecoats bring color to the car. They are applied over the primer surface and covered by the clearcoat layer to protect it from the environment. The flake orientation within the base coat is affected by its composition and the manner in which it is sprayed[3]. In a typical paintshop, the car body enters a topcoat line followed by an external electrostatic bell application to apply the basecoat to the vehicle body. A clearcoat spray is then applied over the basecoat. The clearcoat is responsible for UV protection, chemical resistance, chip resistance and so on. Be sides protecting the basecoat, the polished clearcoat gives a deep lustrous shine to the finish, enhancing its appearance.

2.2 Visual Evaluation of Appearance

The appearance attributes of metallic finishes can be divided into two kinds depending on the viewing distance and illumination conditions. At larger distances of a few meters we observe macro appearance features such as color travel and luster. On the other hand at a closer distance micro features such as the texture or the spatial distribution of color of the finish become more apparent. McCamy[4],[5] in his two comprehensive articles gives a complete description of the appearance and visual attributes of special effect coatings. We now review the terms associated with the visual appearance of metallic coatings .

Color

The color of an automotive finish depends on the kind of pigment used. Three main types of finishes are solid, metallic and interference colors. Conventional solid colors are created by using absorption pigments. The pigment particles give the finish its characteristic color through selective absorption of the incident light. Solid colors remain fairly constant in their appearance and color with viewing and illumination direction. Special effect pigments play a more dominant role in automotive coatings as they enhance the appearance of the car by accentuating its curves. Unlike solid colors, metallic finishes change in brightness with viewing and illumination conditions. In the case of interference coatings, the color hue changes with viewing and illumination direction.

Figure 2.2: Color of an automotive finish. Left: A conventional solid red color has been used to finish the car. Its appearance remains fairly constant with viewing angle and the car appears relatively flat. Right: A similar model of car finished using a metallic gray color. Unlike the solid color, the metallic color changes in brightness with viewing and illumination direction, enhancing the contours and style lines of the car.

Color travel, face and flop

The observed color of a metallic finish is highly dependent on the viewing/illumination direction as well as the illumination conditions. For example, a car painted a metallic green might appear similar to one that is painted solid green under diffused illumination such as a cloudy sky. But under direct illumination such as sunlight, both cars appear remarkably different. The color of the metallic finish varies in brightness, changing from a bright teal color near the specular regions to blackish green elsewhere. This

change in brightness or color travel from bright to dark accentuates the curves of the car. The more rapid the change with viewing angle, the better the curves of the car are accentuated. The light-dark color travel may also be observed by tilting a sample paint panel back and forth. The color observed when the line of sight is along the normal to the surface of the specimen is called the *face* color. The surface is facing the observer. The color observed when the specimen is viewed at a large angle to the normal is called the *flop* color[4]. This change in brightness is influenced largely by the orientation and size of the metallic flakes. When the flakes are oriented parallel to the plane of the coating i.e. parallel to the substrate, it will give a bright reflection at the specular angle and decrease in brightness as the aspecular angular increases. If the flakes are not oriented parallel to the substrate, they will reflect little or no light at usual viewing angles. If a high proportion of flakes have poor orientation, the coating will look dark from all angles and the finish will become unacceptable.
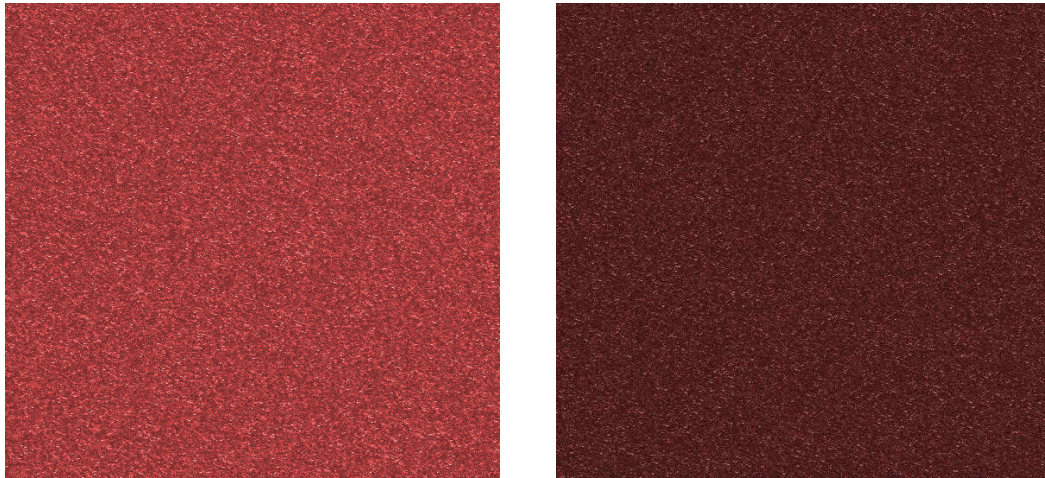
Figure 2.3: Face and flop color of a special effect finish. The orientation of the metallic flakes and the viewing and illumination direction influence the observed color of the coating, resulting in face and flop colors. Left: When viewed along the line of sight, the flakes in the coating are oriented parallel to the plane of the coating and the bright face color of the coating is seen. Right: When the surface is at a large angle to the normal, the flakes reflect little light resulting in a flop color.

Figure 2.4: Luster of an automotive coating. The clearcoat applied on the top of the basecoat gives the surface of the car a lustrous, mirror like finish. Luster causes an angular variation of the amount of light reflected from the surface. At the specular angle, a bright flash is observed and the brightness and saturation of the coating are maximum.

Luster

The clearcoat applied on top of the basecoat gives the finish a lustrous, mirror like finish. Luster is therefore more a property of the clearcoat rather than the basecoat. Luster refers to the variation in appearance with angle caused by a variation in the amount of light specularly reflected from the surface. The reflected light affects the brightness and saturation of the color of the underlying basecoat. The brightness and the saturation are maximum at the specular angle.

Sparkle

Under bright, direct illumination conditions such as bright sunlight the flakes in a metallic finish glitter creating a sparkling effect. Tiny, bright sparkles of light that vary in intensity can be seen, similar to stars in the night sky. This effect is referred to as sparkle. The sparkle is observed only at close distances and is seen only under direct bright illumination. The sparkling effect in metallic finishes is so striking that other
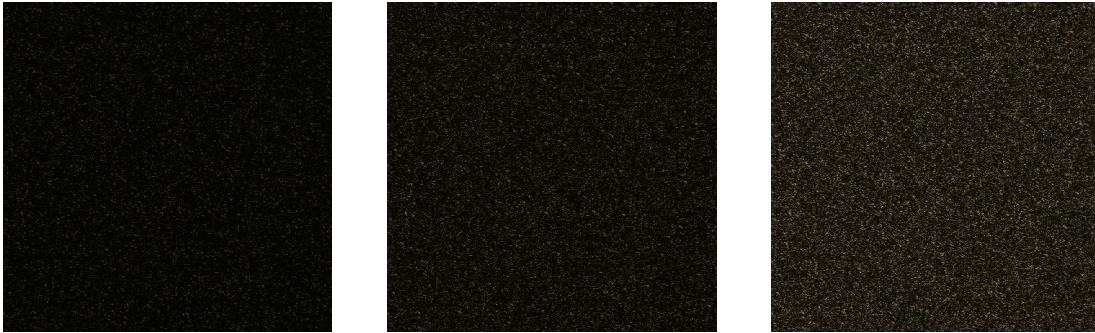
Figure 2.5: Sparkle of a metallic coating. Under bright, direct illumination, the flakes in the metallic finish appear as tiny, bright sparkles of light that vary in intensity, similar to stars in the night sky. As the surface approaches the specular angle, the sparkling effect becomes more intense, as seen above in three different views of the same black metallic coating.

micro appearance aspects are lost while observing it. On the other hand, under diffused illumination such as a cloudy sky, metallic finishes do not sparkle. Instead they may create a salt and pepper, light dark pattern. This effect may be referred to as graininess or coarseness. Both sparkle and graininess depend on the flake size, orientation and distribution[5]. Metallic finishes with larger coarse flakes will show an intense sparkle while those with very fine flakes will appear uniform, almost like a solid color.

Distinctness of Image and Orange Peel

Depending on the viewing conditions and the focus of the observes eye, different visual attributes of the clearcoat are observed. If we focus on the reflected image of nearby objects in the clear coat, we can observe the image forming capabilities of the surface. This aspect of appearance is referred to as distinctness of image. ASTM E 284 defines distinctness-of-image (DOI) gloss as the aspect of gloss characterized by the sharpness of images of objects produced by reflection at a surface[6]. The reflection of the objects may be sharp if the clearcoat has a smooth mirror like finish or blurred if its surface is wavy. The waviness of the surface is affected by the coating substrate as well as the thickness ans evenness of the clearcoat itself. The distinctness of image is also influenced by the color of the basecoat, being more noticeable in darker colors. If the observer's eyes are focused on the surface of the coating itself, another phenomena known as orange peel is sometimes observed. ASTM E 284 defines orange peel as 'the

Figure 2.6: Distinctness of image in an automotive coating. The reflected image of nearby objects is observed when the eye is focused on the surface of the clearcoat. Distinctness of image is the sharpness of these reflected images. Notice how the reflections are enhanced by the presence of a darker basecoat.

appearance of irregularity of a surface resembling the skin of an orange'[6]. A surface with an orange peel effect has many small indentations that appear as a pattern of highlighted and non highlighted areas. These attributes of the clearcoat can also cause the metallic basecoat to be illuminated diffusely. A small amount of haze or surface roughness reduces the visibility of the flakes and the appearance of the sparkle.

2.3   Experimental Data

The data used in the experiments to evaluate the usefulness of the in producing color matches for metallic coatings consisted of two sets of metallic paint panels. The first set consists of metallic black panels, while the second set consists of three subsets of colored panels - red, green and blue. The panels in each set were subjected to visual assessment by color matching experts, performed in a controlled environment. The black metallic set consists of 15 panels which are divided into three subsets of five panels each named A, B and C. The evaluation of the panels by the color matching experts can be summarized as follows: Panels from set A represent the color standard and match each other. Panels from set B match each other, but don't quite match those from set A. Panels from set C do not match each other and are considered a poor match for the panels from set A and B. The second set of panels consists of three subsets of colored metallic panels - red, green and blue. Each subset consists of four panels. The first panel is the color standard. The remaining three panels were subjected to visual assessments, performed in a controlled environment, and were unanimously ranked by three color matching experts, independent of each other as an acceptable(A), borderline (B), or unacceptable match (C) for the standard.
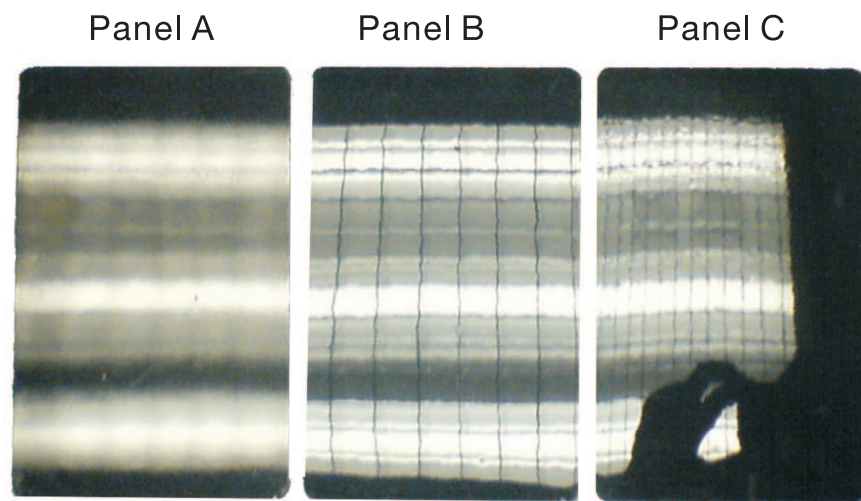
Figure 2.7: Varying distinctness of image and orange peel of three black panels. The waviness of the surface of the clearcoat causes changes in the distinctness of image and observed orange peel for basecoats of the same color. Shown in the figure is a reflection of a fluorescent light fixture seen in the panels. Notice that while the reflected image appears hazy in sample A, it is distinct in samples B and C. The orange peel effect is clearly seen when one observes the roughness of the grid like pattern of the fixture reflected in Panel C.

Figure 2.8: Paint Samples used in the Matching Experiments. The samples consist of metallic black, red, blue and green panels as seen in the figure. Each set of panels was evaluated visually by color matching experts and consists of a color standard, a close match, a borderline match and an unacceptable match

2.4   Current Matching Methods

Metallic finishes are visually complex. Besides an angular dependency of color and brightness, they also exhibit luster, sparkle etc. As a result of these visual attributes matching two metallic coatings is a challenge. Color theory is still not fully developed for effect coatings and so the final match relies on the visual judgement of a color matching expert. Current methods of color matching are therefore a combination of physical measurements as well as judgement by the trained eye of a color matching expert. We now summarize the various methods used to determine a match for a metallic effect coating.

Color chips

The use of color chips is one of the most commonly used methods to produce a match for a metallic coating. Autobody shops predominantly use decks of color chips to arrive at a color match to repair a finish that has been damaged. The first step in this method is to retrieve the color code for the finish on the vehicle. Each vehicle is tagged with a color code that can be retrieved using the vehicle identification number (VIN). The color code indicates the paint that was used to finish the car while on the assembly line. However for each color code there are multiple formulas that provide a match that is acceptable by the vehicle manufacturer. This results in a number of variants for a particular code. To provide a match, after identifying the color code, it is entered into a paint formula database and a prime formula is displayed. Formulae for all known variants are also displayed. To determine which particular variant matches the finish to be repaired, the surface of the vehicle is first cleaned thoroughly. After cleaning, color chips of each variant which are supplied in decks by the paint manufacturer are held next to the vehicle body to check for a color match. The chip that best matches the actual color on the vehicle is then used to find the paint formula for meeting the right paint color. This subjective method however is both time consuming and error prone. Since the chip is placed flat against the vehicle's surface, it is seen from a single viewing direction. Metallic and other special effect pigments change in appearance with viewing

direction. So although the paint may look like a match from a few viewing directions, it may not match the original coating from other directions.

Multi angle Spectrophotometers

Metallic and special effect coatings change in appearance with viewing and illumination direction. To match special effect pigments, their reflectance must be measured at a large number of viewing and illumination angles. This is not practical for most commercially available devices. Research by the American Society for Testing and Materials (ASTM)(sub-committee E12.12, Metallic and Pearlescent Colors) and the Deutsches Institut fur Normung (DIN) determined a minimum of three and preferably five viewing angles with a fixed illumination direction as the standard for matching metallic finishes[6],[7],[8]. To characterize the finish, the near specular angle(15), the face angle(45), and the flop angle(110) with a $45°$ illumination angle were determined to be of major importance. Based on these specifications, a number of spectrophotometers are available and are commonly used for color matching of metallic finishes. These instruments however often do not provide an accurate color match. Because of the small number of viewing angles used for measurement the spectrophotometers are unable to correctly characterize the brightness/color travel of special effect pigments. Furthermore, metallic coatings not only change in appearance with viewing angle, but also illumination conditions: direct sunlight versus cloudy sky or artificial lighting. The sparkling effect of the finish cannot be captured with currently available multiangle spectrophotometers. This limitation is because they measure the integral of spectral reflection over an area and cannot distinguish between the basecoat color and the reflection of the flakes. They also cannot determine changes in the overall appearance of the coating due to the clearcoat (such as orange peel). Investigations by paint manufacturers into effect coatings comprising the latest generation of special effect and interference pigments using a wide variety of measuring instruments such as the multiangle spectrophotometer have indicated that currently available color measuring instruments do not entirely reproduce the visual impression of these pigments[9]. Color technicians therefore rely on these devices to provide only an initial guess for the

color match and then rely on visual techniques to arrive at the final color.

Chapter 3

BTF based matching

3.1 Introduction

In recent years, the use of special effect pigments, especially metallics in automobile finishes has become popular. These pigments are a combination of colored particles along with innovate substrates like mica or aluminum flakes or more recently multilayer interference flakes. Newer pigments such as Xirallic exhibit an intense sparkle effect when viewed under direct sunlight. This sparkle is also seen in the other metallic effect coatings under intense direct illumination such as sunlight. Besides the sparkle, some finishes also show a salt and pepper like appearance under diffused or cloudy conditions. The surface texture and luster of the clear coat also adds to the visual complexity of the coating. With automobile manufacturers establishing stringent color matching standards, traditional methods of visual color matching evaluation are no longer acceptable. Nor can the appearance based characteristics of the coatings be captured nor sufficiently characterized by traditional 5-angle color measurement. We therefore propose a new BTF based matching method that takes extends color-based matching to account for appearance variations with viewing and illumination. This extension better represents characterizes appearance characteristics such as brightness, sparkle and surface texture. This method is shown to have a high correlation with the visual judgement of color matching experts.

3.2 Bidirectional Texture Function

The appearance of an automotive finish depends on view, illumination and scale at which the surface is observed. Accurately capturing their appearance requires measurement of light reflected from the surface as a function of viewing and illumination direction. Reflectance of a surface as a function of viewing and illumination angle is described by the surface's bidirectional reflectance distribution function (BRDF). Since the BRDF of each finish is unique, it can be used as a match measure to differentiate between coatings that closely resemble each other.
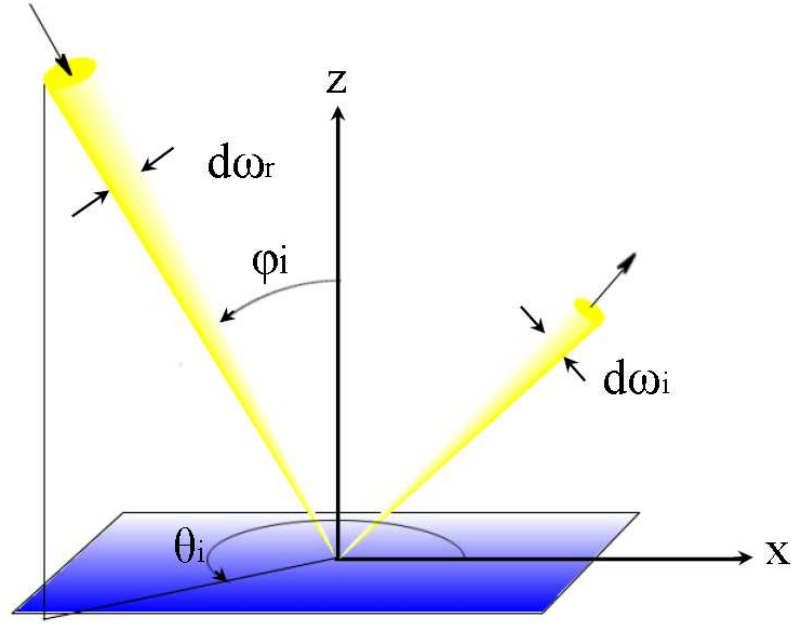
Figure 3.1: [Definition of the BRDF.]

The BRDF is formally defined as the radiance reflected by a scene point divided by the irradiance and can be written as

$$f\left(\theta_i, \phi_i; \theta_e, \phi_e\right) = \frac{\delta L\left(\theta_e, \phi_e\right)}{\delta E\left(\theta_i, \phi_i\right)}, \tag{3.1}$$

where θ_i and ϕ_i are the polar and azimuthal angles of illumination direction respectively, and θ_e and ϕ_e are the polar and azimuthal angles of viewing direction, respectively[10],[11]. Measurements of the BRDF are useful in characterizing uniform or homogeneous materials that exhibit negligible variation in their reflectance properties along the entire

surface. However, most real world surfaces have spatially varying material properties, i.e. they have some sort of texture which the BRDF fails to capture. The extension of the BRDF that captures this spatial variation is called the bidirectional texture function (BTF), a 6D function characterized by 2D surface position as well as viewing and illumination direction[12]. The BTF can be written as $f(x, y, \theta_i, \phi_i, \theta_e, \phi_e)$. The BTF is essentially a texture that changes in appearance with viewing and illumination direction. Because the BTF can capture complex effects such as shadowing, masking etc besides the angular variation in appearance of a surface, it is well suited for capturing the appearance of a visually complex material such as metallic paint.

3.3 BTF Measurement

Measurement of the BRDF requires sensing light reflected from an image point as a function of viewing and illumination direction. The camera and light source must be positioned in all possible combinations of viewing and illumination directions. For both the camera and the light source, the set of all possible viewing directions is a hemisphere above the surface point. With viewing and illumination directions varying over a hemisphere, measurement setups can be quite complex to enable precise angular variations of both viewing and illumination directions. Furthermore, to measure a spatially varying BRDF (i.e. BTF) added equipment complexity is necessary for sensing a region instead of a surface point. The most common approach to measure the BTF is to use a gonioreflectometer- like setup with a CCD-chip instead of a spectrometer. The term BTF was first introduced in the CUReT[12]. measurement study that used a gonioreflectometer-type system to capture the appearance of 3D surface textures.The measurement method in this study had the disadvantage of being time consuming, semi-automated and required mountable planar patches of the surface of interest. In many applications, such isolated patches are difficult or impossible to obtain. Other arrangements such as a hemispherical gantry with a large number of mounted cameras and light sources are capable of measuring many samples in a short time, but are complex and costly to build[13]. Instead we make use of the Texcam as described in [14][15][16] that uses off the shelf components and a simple imaging procedure. The

Texcam uses a concave parabolic mirror to capture multiple views of the same surface point simultaneously, allowing more rapid data acquisition, while simultaneously controlling illumination direction. Planar translations of the surface to be measured are used for capturing the BTF, as opposed to hemispherical positioning of the camera and light source relative to the sample.

3.3.1   Device Design

We now repeat the important design features of the Texcam that are relevant to this work, as described in [14][15][16]. The Texcam uses off the shelf optical components such as a beam splitter, a concave parabolic mirror, a CCD camera, and translation stages and is shown in Figure 3.2 . The beam splitter allows simultaneous control of viewing and illumination direction. A concave parabolic mirror section is positioned so that its focus is coincident with the surface point to be measured. The illumination source is a collimated beam of light parallel to the global plane of the surface and passing through a movable aperture. The aperture ensures that only a spot of the concave parabolic mirror is illuminated, and so one illumination direction is measured for each aperture position. In this approach, the problem of changing the illumination direction over a hemisphere is transformed to the easier problem of translating an aperture in a plane. Because the surface point is at the focus of parabolic mirror, the light reflected by the surface point at each angle is reflected from the mirror to a parallel direction and diverted by the beam splitter to the camera. The camera is equipped with a telecentric lens that images the light parallel to the optical axis. The image of the mirror is viewed by the camera that is positioned in such a way that its optical axis lies along the Y axis so that a single image corresponds to reflectance measurements over a partial hemisphere. This arrangement has the advantage that all light from the measurement point will reflect away from the sample and thus will not reilluminate the surface point, thereby changing the intended illumination pattern. The Texcam image of a piece of blue glossy cardboard is shown in Figure 3.4.
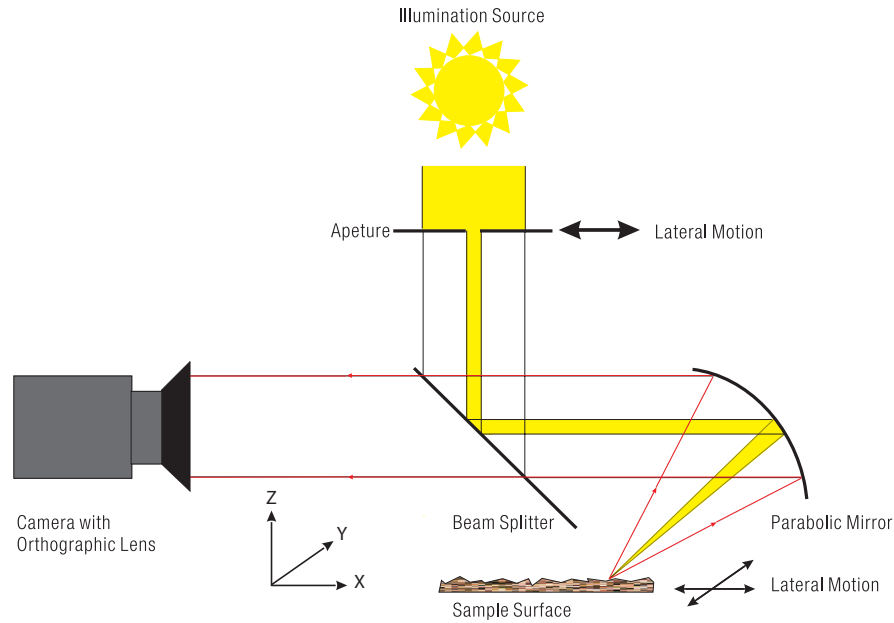
Figure 3.2: BRDF/BTF Measurement Device. The surface point is imaged by a CCD video camera observing an off-axis concave parabolic mirror to achieve simultaneous observation of a large range of viewing directions. The device achieves illumination direction variations using simple translations of the illumination aperture. Measurements of bidirectional texture are accomplished by translating the surface in the X - Y plane.
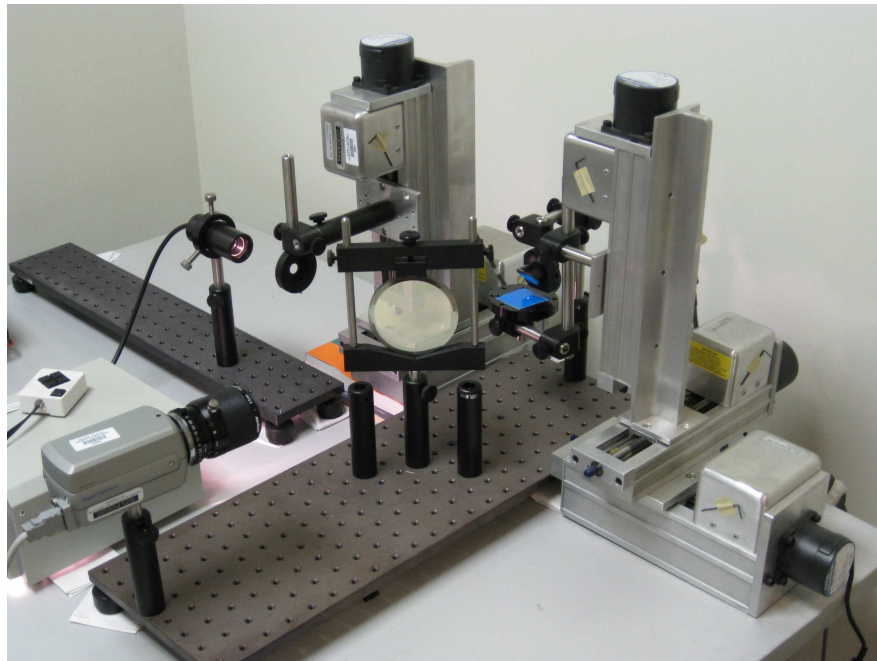
Figure 3.3: Prototype Implementation of the Texcam. The prototype device has an off-axis parabolic mirror (A8037-175, Janos Technology), a Fiber- Lite PL 900 collimated illumination source, and movable aperture and sample stage using Velmex Bislide stepper motors and a Sony DFW500 camera fitted with a telecentric lens.

Figure 3.4: Instantaneous multiple view images. The Texcam is able to image all views of a point on the sample surface within a partial hemisphere simultaneously within a single image. Information about the surface such as the specularity, body color etc. are all obtained instantaneously through the same image. Left: The Texcam image (i.e. the BRDF) of a piece of glossy blue cardboard. Right: Texcam image of blue metallic paint. No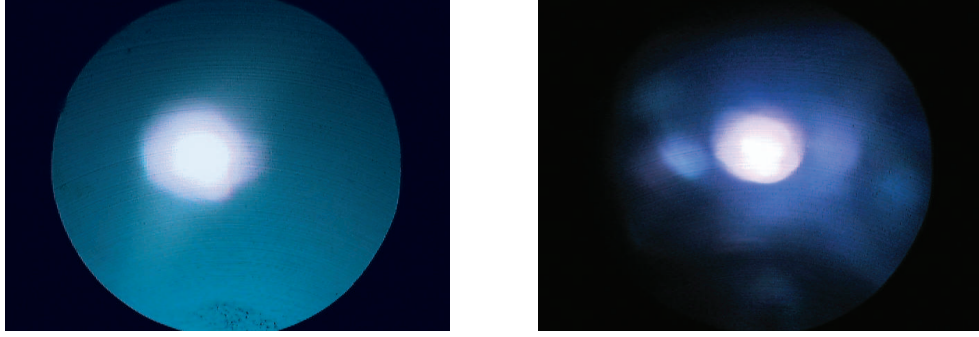tice how the BRDF of the metallic paint is complex. Besides the primary specularity and the blue body color, the flakes in the paint also produce secondary peaks in the image.

3.3.2   Prototype Implementation

The prototype device has an off-axis parabolic mirror (A8037-175, Janos Technology) that is a section of a full parabolic mirror and extends from point A to point B as illustrated in Figure. The equation for the surface of the parabolic mirror as shown in Figure 3.5 is

$$y + F = \frac{z^2 + x^2}{4F}, \tag{3.2}$$

where F is parent focal length (12.7 mm for the current prototype). This function is obtained by rotating the parabolic curve $y + F = \frac{z^2}{4F}$ about the Y axis. The image of the mirror is viewed by the camera (through a telecentric lens) that is positioned so that its optical axis lies along the Y axis. The point on the mirror with coordinates $x = 0$, $y = 0$, $z = 2F = 25.4$ mm is the point in the center of the projected image.

Since the radius of the projected image is 12.7 mm, we can easily calculate the coordinates of B in Figure 3.5 as
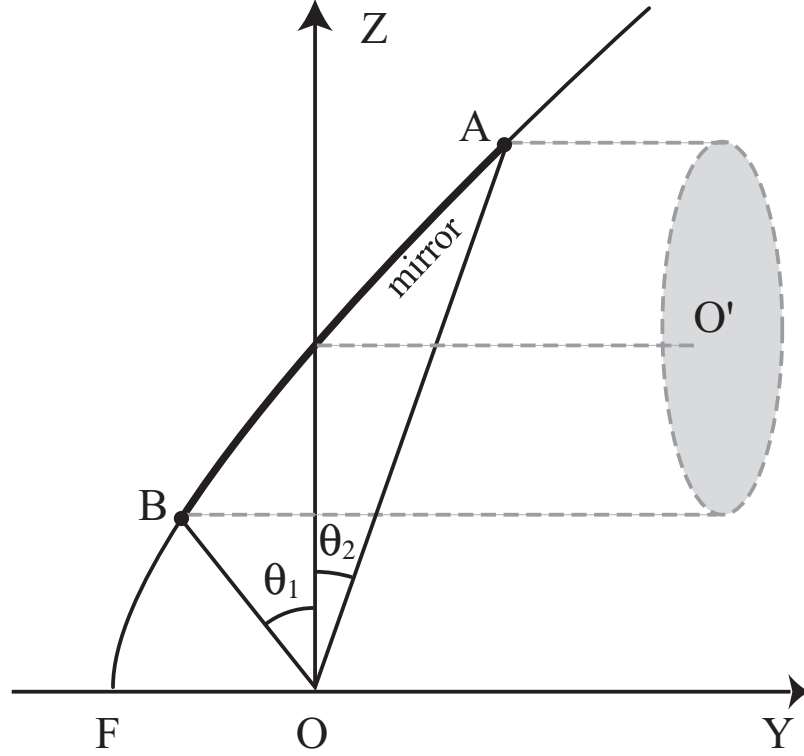
Figure 3.5: Parabolic mirror used in the Texcam prototype. The mirror is a section of a full parabola that extends from point A to point B. Light reflected from the surface point at the focus of the mirror is reflected parallel to the optical axis and forms the circular projected image with center O. Image reproduced from [14] with the permission of the author.

$$
\begin{aligned}
z_B &= 12.7 = F, \\
y_B &= \frac{z^2 + x^2}{4F} - F = -\frac{3}{4}F.
\end{aligned}
\tag{3.3}
$$

The angle θ_1 is

$$
\theta_1 = \arctan(\frac{3}{4}) = 36.8^o.
\tag{3.4}
$$

By the same method, the coordinates of A in Figure 3.5 are expressed as

$$
\begin{aligned}
z_A &= 3 \times 12.7 = 3F, \\
y_A &= \frac{z^2 + x^2}{4F} - F = \frac{5}{4}F.
\end{aligned}
\tag{3.5}
$$

The angle θ_2 is

$$\theta_2 = \arctan(\frac{5}{4}) = 22.6^o. \tag{3.6}$$

Note that the camera image is a circle of 25.4 mm diameter and is the view looking down the Y axis. Since the image is 640×480 pixels and the diameter size in the screen is 486 pixels, each pixel in the camera image represents the physical size $p = 25.4/486 = 0.052$ mm. The transformation from screen coordinates x_s, y_s to the real world coordinates shown in Figure 3.5 is straightforward,

$$x = -(x_s - C_x) \times p \tag{3.7}$$

$$z = -(y - C_y) \times p + 2F \tag{3.8}$$

$$y = \frac{(x^2 + z^2)}{4F} - F. \tag{3.9}$$

where Cx and C_y are the center of the screen, for the 640×480 setting, $Cx = 319, C_y = 239$, F is parent focal length (12.7 mm for the current prototype) and p is the physical pixel size, $p = 0.052$mm.
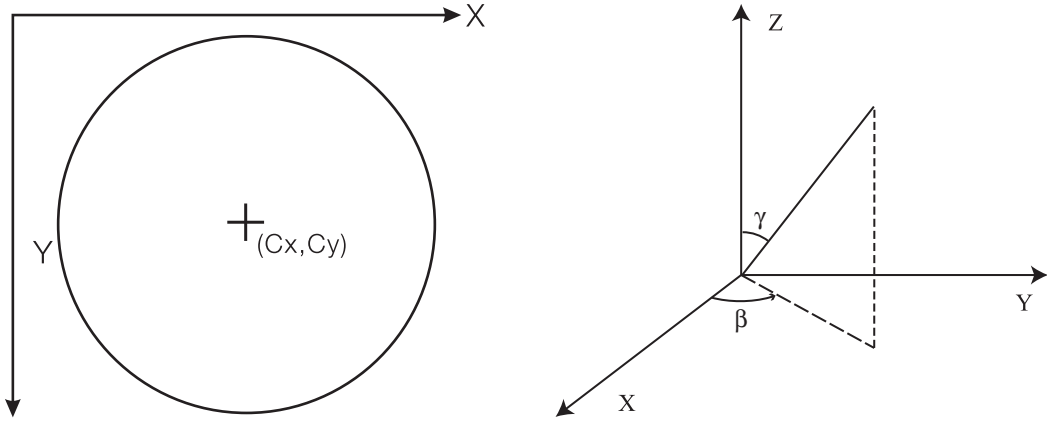

Figure 3.6: Conversion from screen coordinates to real world coordinates. The XY coordinates of a pixel in the Texcam image are easily converted to their corresponding viewing and illumination directions in terms of polar and azimuthal angles.

The corresponding polar and azimuthal angles are given by

$$\gamma = \arccos(\frac{z}{\sqrt{x^2 + y^2 + z^2}}) \tag{3.10}$$

$$\beta = \arccos\left(\frac{x}{\sqrt{x^2 + y^2}}\right) \tag{3.11}$$

where γ and β are the polar and azimuthal angles respectively, as seen in Figure 3.6.

3.3.3   Imaging Procedure

The BTF of the metallic paint sample is obtained through planar translations of the sample surface. The size of the texture image pixel, is therefore controlled by the movement of the surface. The stage controlling the movement can be made to move in very small increments (0.0025mm for the current prototype), although the optical imaging principles limit the system resolution. The maximum physical size of each pixel is 0.052mm. To obtain the BTF, the illumination aperture is positioned to achieve the correct illumination direction. The surface is then translated along a two dimensional grid in the X-Y plane and Texcam image (i.e. the BRDF of the surface point) is stored for each translation. A sample of these Texcam images are shown in Figure 3.7. The spatial variation in the BRDFs of successive surface points is clearly seen in the figure. This spatial variation occurs due to the inhomogeneous composition of the finish. The bright specularity at the center is caused by the glossy clearcoat, the blue pigment imparts a blue body color to the BRDF while the secondary peaks are caused by the presence of the tiny metallic flakes within the coating. A pixel that corresponds to the desired viewing direction is then acquired for each surface position from the set of Texcam images. The pixels thus selected are put together in the same sequence as the surface was translated to obtain the reconstructed surface texture image, for one viewing direction. This procedure is illustrated in Fig3.8. To obtain a texture image from a different viewing direction, a pixel from a different location in the Texcam image is chosen. The texture images from such viewing directions are arranged sequentially to form the BTF of the paint sample. An example of these texture images and their corresponding viewing angles is shown in Fig 3.9. The different views the surface patch are the stitched together to form a composite multiview image. The advantage of stitching the views together in a sequential manner is that it produces registered multiview images that can then be used to analyze the visual characteristics of the

coatings.
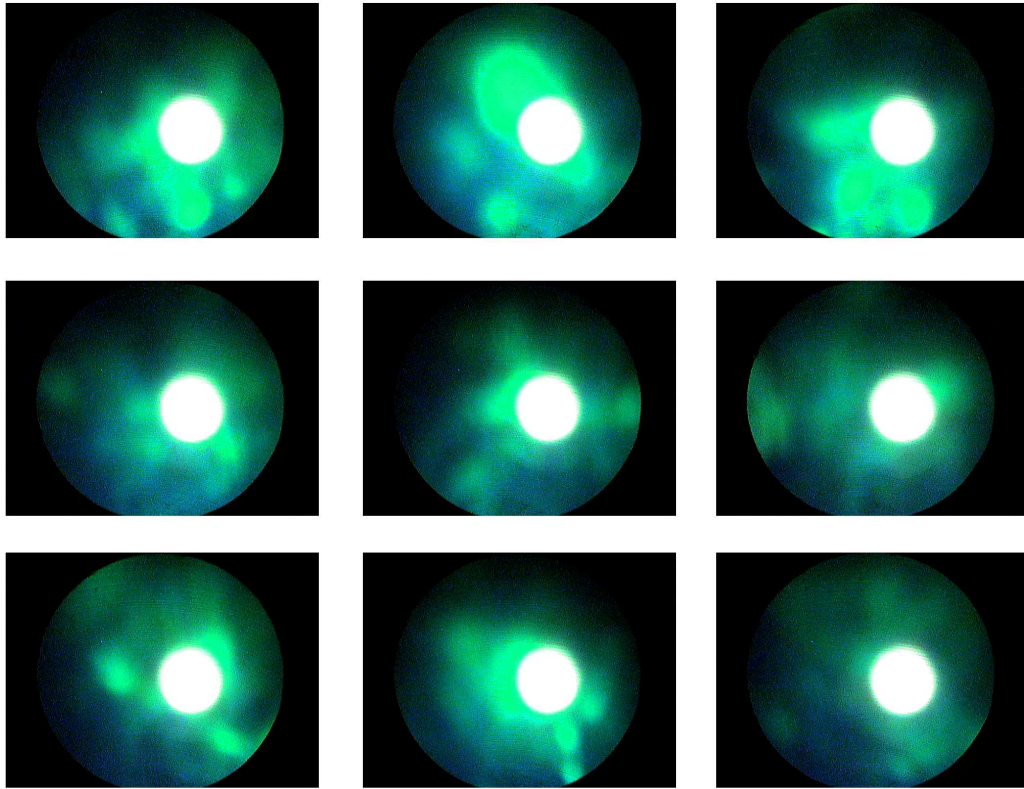
Figure 3.7: Texcam Images of a Metallic Green Paint Sample. Seen in the figure are the Texcam images for six successive spatial points on a metallic green paint panel. Notice how the reflectance of the points changes due to the inhomogeneous composition of the paint. The bright specularity at the center of the image is caused by the glossy clear coat. Also seen in the images are the green body color due to the green pigment and the secondary specualrities caused by the metallic flakes in the paint.
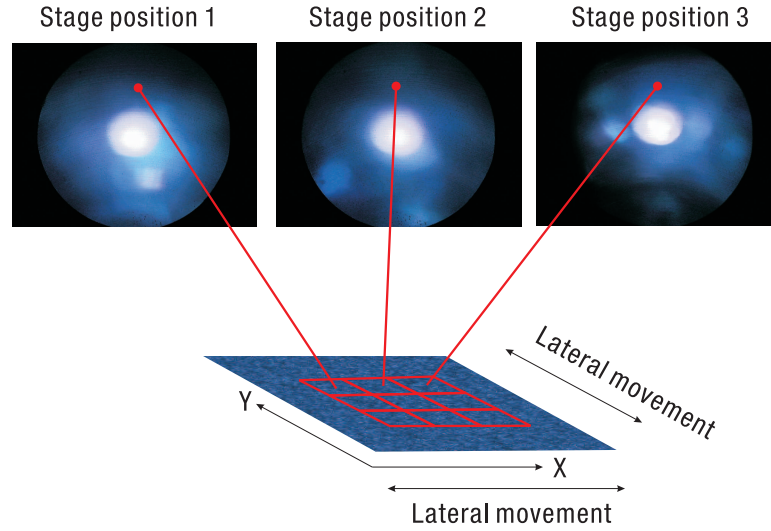
Figure 3.8: Imaging Procedure of the Texcam. A viewing direction is selected by choosing the appropriate pixel from the multiview image. The surface to be scanned is then translated along the X- Y plane and several such pixels from each the multiview image are put together in the scanning sequence to produce a spatial reconstruction of the surface as seen from that viewing direction.
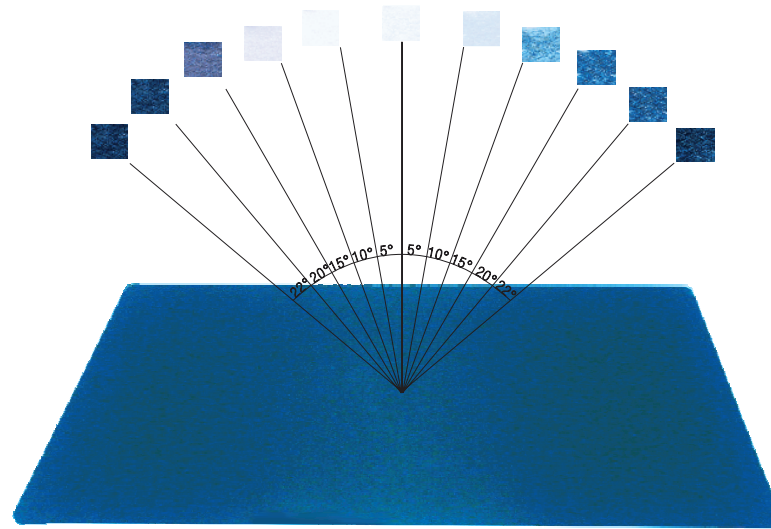
Figure 3.9: An illustration of the viewing directions that are reconstructed by the camera. Shown in the figure are the spatial reconstructions of the square patch of the panel as the polar angle is changed. 50 viewing directions are captured; the first 25 are for a fixed azimuth angle of $-90°$ with the polar angle varying from $0°$ to $24°$ in increments of $1°$, and the next 25 are for a fixed azimuth angles of $+90°$ with the polar angle varying from $0°$ to $22°$ in increments of $1°$. The square patch on the extreme left would therefore correspond to a viewing direction that has a polar angle of $24°$ and an azimuth angle of $-90°$, while the square patch on the extreme right would correspond to a viewing direction that has a polar angle of $22°$ and an azimuth angle of $90°$.

3.3.4 Matching Procedure

Using the procedure described above, the Texcam was used to reconstruct a 5mm$times$5mm patch of each of the panels as seen from 50 different viewing directions. The different views of the patch were then put together in sequence to form a composite spatial reconstruction. The advantage of such a composite spatial reconstruction is that it allows all the visual characteristics of the coatings to be visualized simultaneously. The precise color travel of the coating, surface texture, primary specularity and sparkle due to the flakes may all be observed in a single image, as seen in Figure 3.10. The sequence of different viewing directions of the panel represents the color travel of the coating. The color travel is quantified as the BRDF of the coating and BRDFs of different coating can be compared to determine whether they match each other. Such a BRDF curve for a black metallic paint sample and its corresponding multiview image is shown in Figure 3.11. It is important to note that unlike a conventional multi- angle spectrophotometer, reflectance measured by the Texcam is independent of the placement and orientation of the panel [17]. To determine whether a colored coating matches the standard or not, we first find the the average RGB value for the patch for each viewing direction. The images are intensity normalized and thresholding is used to remove the saturated measurements that occur close to the specularity. The difference in the RGB components for each viewing direction gives the error between the sample panel and the standard and is used to determine the goodness of the match.
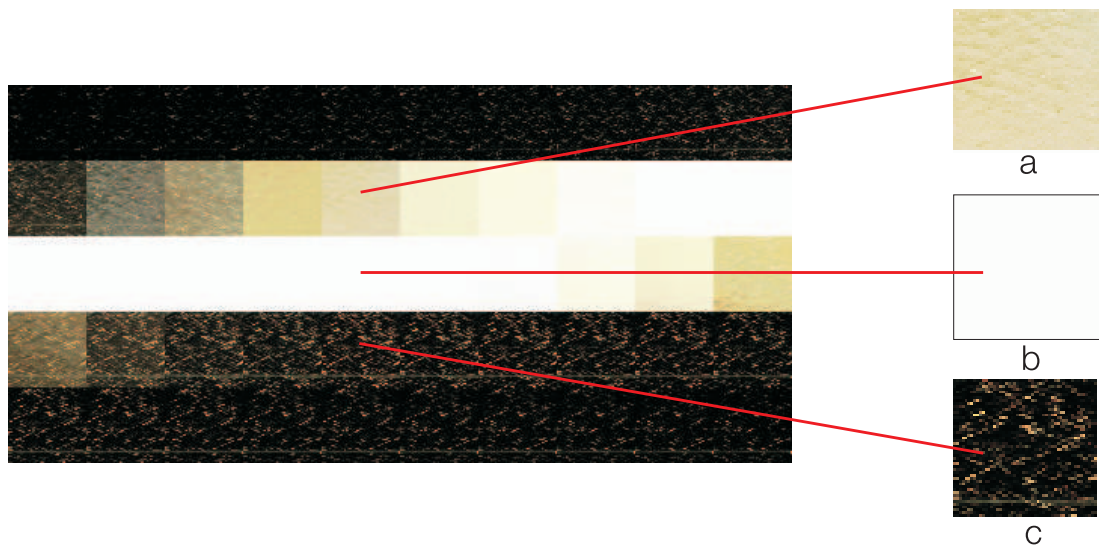
Figure 3.10: The spatial reconstruction of a square patch from a black panel showing its three distinct components.(a): surface texture (b): primary specularity (c): subsurface reflectance. Note the sparkle that is observed in the subsurface reflectance; also note that an *orange peel* effect is visible in the surface texture. The measurements differ in texture appearance indicating that the Texcam is capable of imaging each component distinctly. Each square represents a different view of the same patch. When viewed as a sequence, the spatial reconstruction shows the precise change in color with viewing direction.
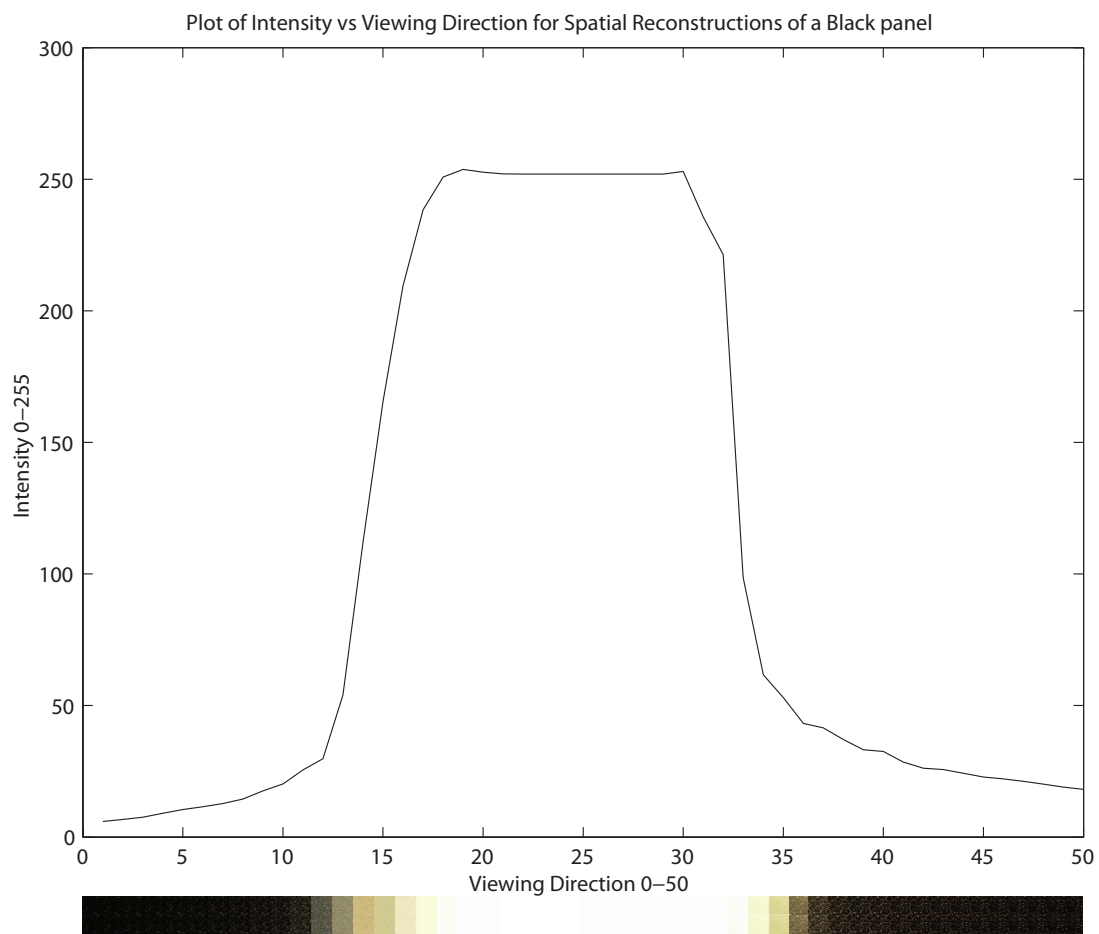
Figure 3.11: The BRDF of a Metallic Black Panel. The measured intensity of a black metallic coating is plotted as a function of viewing direction. Shown below the plot are the corresponding views of the surface patch. This BRDF curve represents the precise change in brightness of the coating with angle and can be used as a match measure to quantitatively compare it with other coatings.

3.4 Experimental Results

The goal of the experiments performed using metallic coatings was to evaluate the usefulness of the Texcam in producing color matches that showed a high correlation with the visual judgement of color matching experts. Two sets of panels have been used in the experiments. The first set consists of metallic black panels, while the second set consists of three subsets of colored panels - red, green and blue. The panels in each set were subjected to visual assessment by color matching experts, performed in a controlled environment. The panels were then imaged by the Texcam and matched based on their reflectance measurements across multiple viewing directions, to determine whether the matches produced by the Texcam agreed with those of the color matching experts.

3.4.1 Experiment 1

The first experiment consisted of matching 15 metallic black panels. The panels are divided into three subsets of five panels each named A, B and C. The evaluation of the panels by the color matching experts can be summarized as follows: Panels from set A represent the color standard and match each other. Panels from set B match each other, but don't quite match those from set A. The Panels from set C do not match each other and are considered a poor match for the panels from set A and B. The set of black panels was then studied with the Texcam using the BRDF based matching technique. Figure 3.11 shows a plot of the BRDF of a black panel. Panels that have the same color travel will have similar shaped BRDF curves. We therefore overlap and compare the curves of different panels to classify them into the sets A, B and C. Figure 3.12 shows the BRDF curves for the panels of set A, B and C. Note that although the curves for panel A1 and A3 have the same shape as the rest of the panels in the set, they appear to be displaced toward the right. This is due to warping of the panels. The curves indicate that all the panels from set A match each other. The BRDF curves for the panels of set B overlap each other almost perfectly and hence all panels from set B match each other. The BRDF curves for the panels from set C do not overlap with each other indicating that the panels from set C do not match other panels within the

same set. Furthermore, when the BRDF curves of sets A, B and C are overlapped, as shown in Figure 3.13, it is clear that the panels from set A nearly match set B, but those of set C do not match B at all. These observations are in direct agreement with the experts opinion.
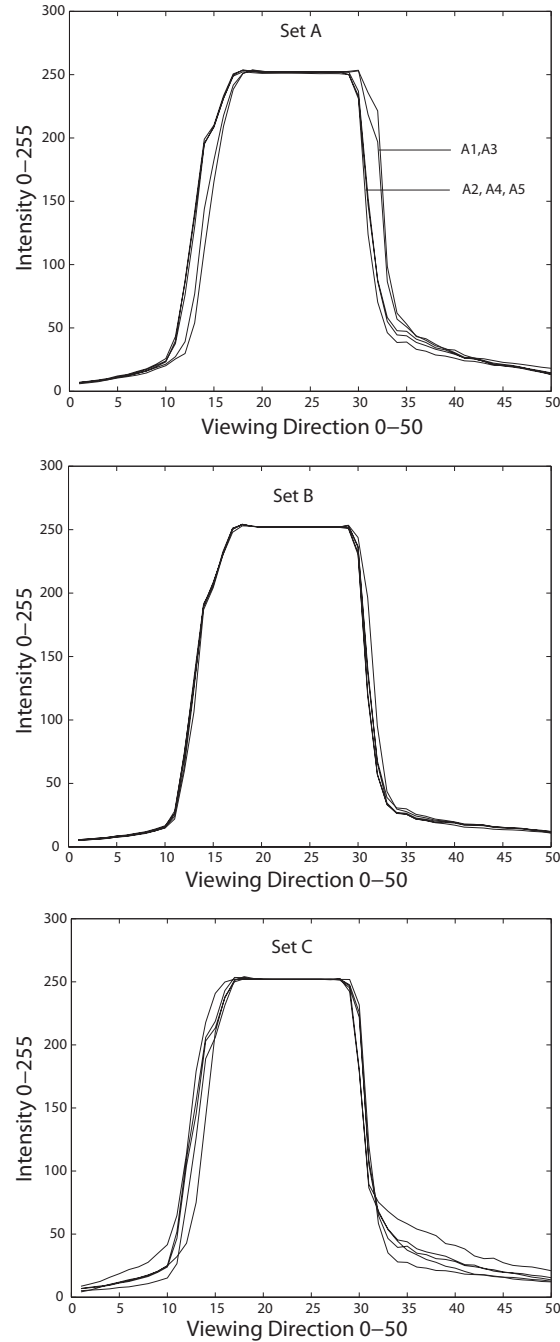
Figure 3.12: Plot of the logarithm of the average RGB value against viewing direction for the sets of black panels A, B and C. The viewing directions are shown in Figure 3.9. The peak represents the brightness observed when the panel is viewed at the specular angle, which then drops off on either side as the viewing direction moves away from the specular angle. Notice that in the BRDF curves of panels belonging to set A, A1 and A3 are displaced to the right of those of A2, A4 and A5. This is due to the warping of panels A1 and A3. The characteristic shape of the BRDF however, remains unchanged. All the panels in set B have the same color and appearance. They match each other perfectly as seen by their overlapping BRDF curves. The non overlapping BRDF curves of the panels in set C on the other hand suggest that they do not match each other in appearance.
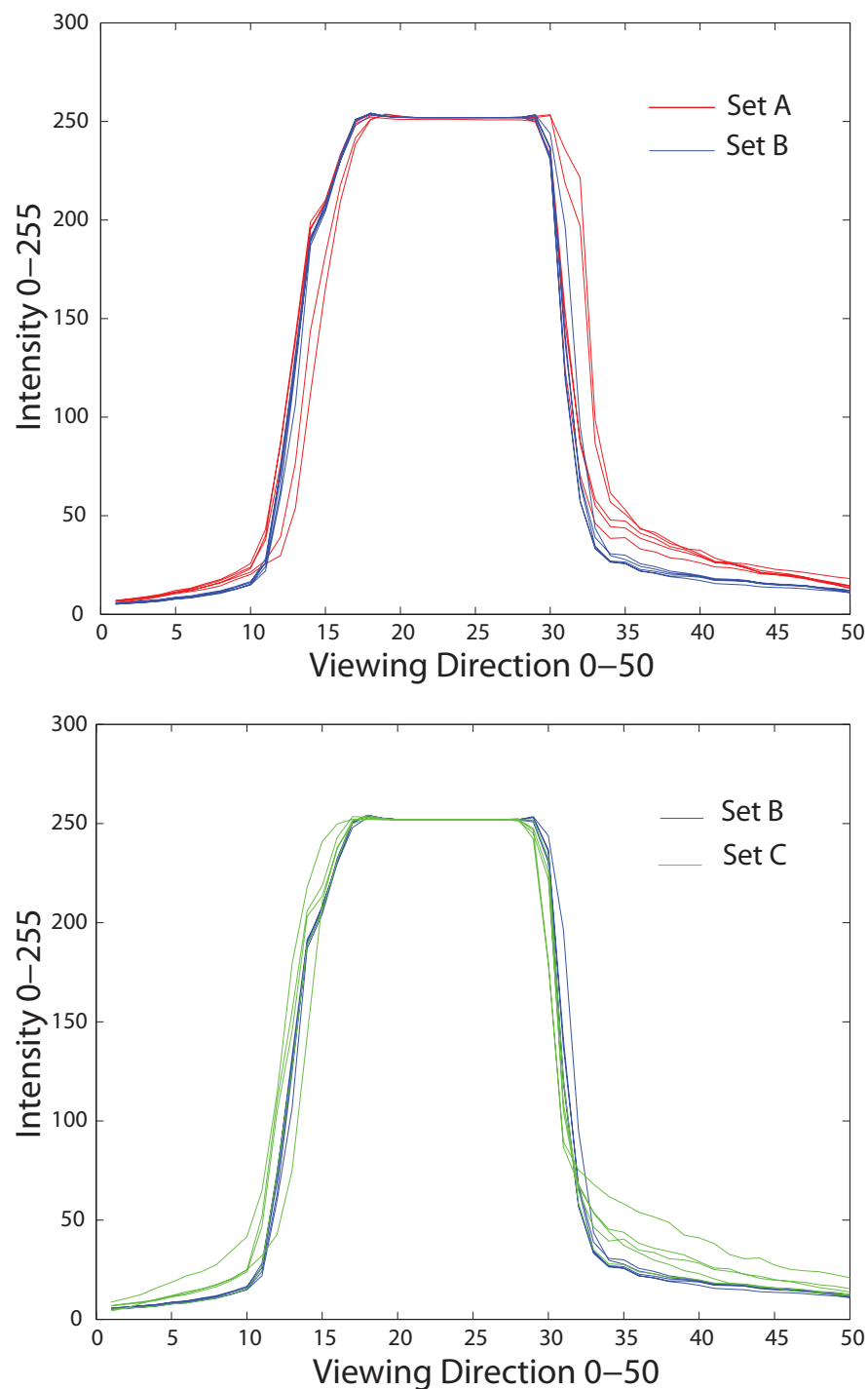
Figure 3.13: Left: Plots of the logarithm of the average RGB value against viewing direction of set A vs those of set B. Right: Plots of the logarithm of the average RGB value against viewing direction of set B vs those of set C. Notice that the panels of set B do not match those of A, although they match the other panels within the set. Similarly, panels from set C do not match those in set B, nor do they match each other. The difference in the characteristic curves is in agreement with the opinion of the color matching experts regarding which panels match each other.

3.4.2 Experiment 2

The second experiment involved the matching of colored panels using the Texcam. Three sets of colored panels were used - red, green and blue. Each set consists of four panels. The first panel is a color standard. The remaining three panels in each set were subjected to visual assessments, performed in a controlled environment, and were unanimously ranked by three color matching experts independent of one another, as an *acceptable* (A), *borderline* (B), or *unacceptable* (C) match for the standard.

Our first set of colored panels analyzed using the Texcam is the metallic red color. Figure 3.14 shows a plot of the RGB error versus viewing angle. Panel C is clearly an unacceptable match and shows a large error across most of the viewing directions. Visual evaluation confirms that it indeed appears darker than the standard on flop. The error in viewing directions 12 through 15 for Panel B indicates that the color travel from light to dark occurs slightly later as compared to the standard. Panel B can therefore be considered as a borderline match.Panel A shows negligible error across all viewing directions, indicating that it has the correct color and travel, and so is an acceptable match for the standard.

The second set of panels is a metallic green color. As seen in Figure 3.15 Panel A and B show a significant error in viewing directions 14 through 17. This indicates that the color travel for these panels slightly differs from the standard. Apart from this minor difference in the color travel, panel A does not show a significant error for the flop color and is an acceptable match when compared to the color standard. Panel B shows some error in flop color for a few viewing directions and is therefore a borderline match for the color standard. Panel C shows the same color travel as the standard, which is reflected in the insignificant error for viewing directions 14 through 17. Panel C does however, show a significant error between viewing directions 20 through 50, indicating that it does not match the color standard in its flop color. Panel C is therefore an unacceptable match for the standard.

The third set of panels is a metallic light blue. As seen in Figure 3.16Panel A shows a large error for viewing directions 20 through 50, This indicates a mismatch in flop

color. Visual evaluation confirms this, with panel A being lighter in color as compared to the standard. The error plot for viewing directions 12 through 15 however indicates that it does show the same color travel. Panel B shows an error in viewing directions 12 through 15 indicating a slight difference in color travel from light to dark. It also does not show a large error in viewing directions 20 through 50, indicating that it is similar in flop color to the standard. Panel B can therefore be regarded a borderline match. Panel C shows a large error in flop color, which can clearly be seen by noticing the error plot for Panel C between viewing directions 20 through 50. Panel C is therefore an acceptable match for the color standard.

Figure 3.14: RGB error versus viewing direction for a set of OEM red panels. Panels A, B and C are the acceptable, borderline and unacceptable match as ranked by the color matching experts. An error for viewing directions 12 through 17 indicates that the panel shows a different color travel while an error for viewing directions 20 through 50 indicates a difference in the flop color of the panel as compared to the standard. C is clearly the unacceptable match, since it has a different flop color as compared to the standard, indicated by error peaks for almost all viewing directions. B shows an error for viewing directions 12 through 17, indicating that it has a slightly different color travel as the standard, but the same flop color. It is therefore a borderline match. A shows the least error across all viewing directions, indicating that it has the same color travel and flop color as the standard. Panel A is therefore an acceptable match.
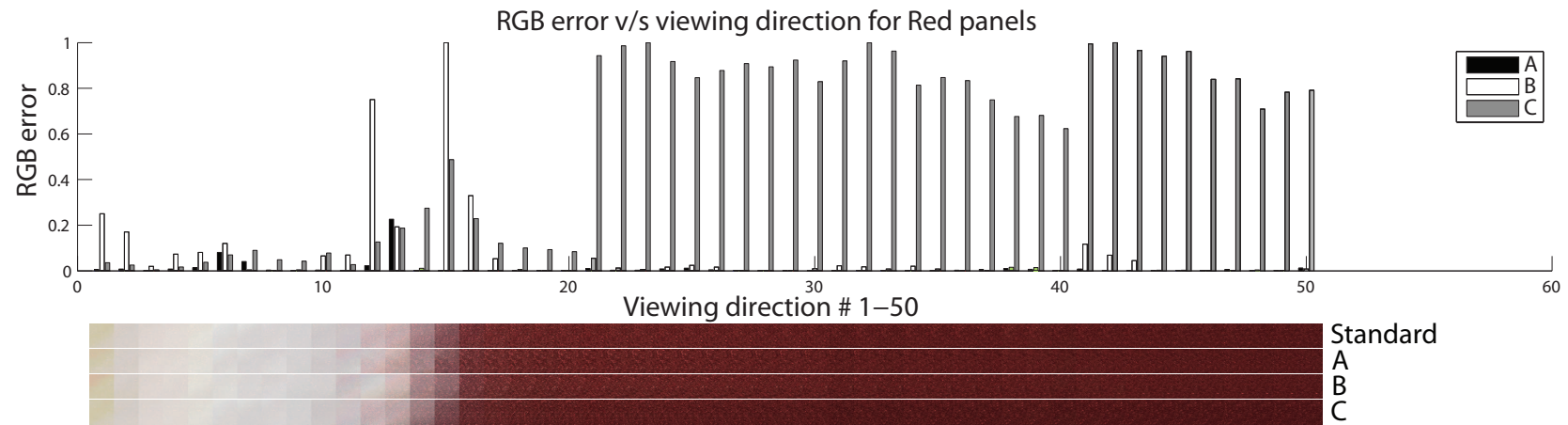
Figure 3.15: RGB error versus viewing direction for a set of OEM green panels. Panels A, B and C are the acceptable, borderline and unacceptable match as ranked by the color matching experts. An error for viewing directions 12 through 17 indicates that the panel shows a different color travel while an error for viewing directions 20 through 50 indicates a difference in the flop color of the panel as compared to the standard. C is clearly the unacceptable match, since it has a different flop color as compared to the standard, indicated by error peaks for almost all viewing directions. B shows an error for viewing directions 12 through 17, indicating that it has a slightly different color travel as the standard, but the same flop color. It is therefore a borderline match. A shows the least error across all viewing directions, indicating that it has the same color travel and flop color as the standard. Panel A is therefore an acceptable match.
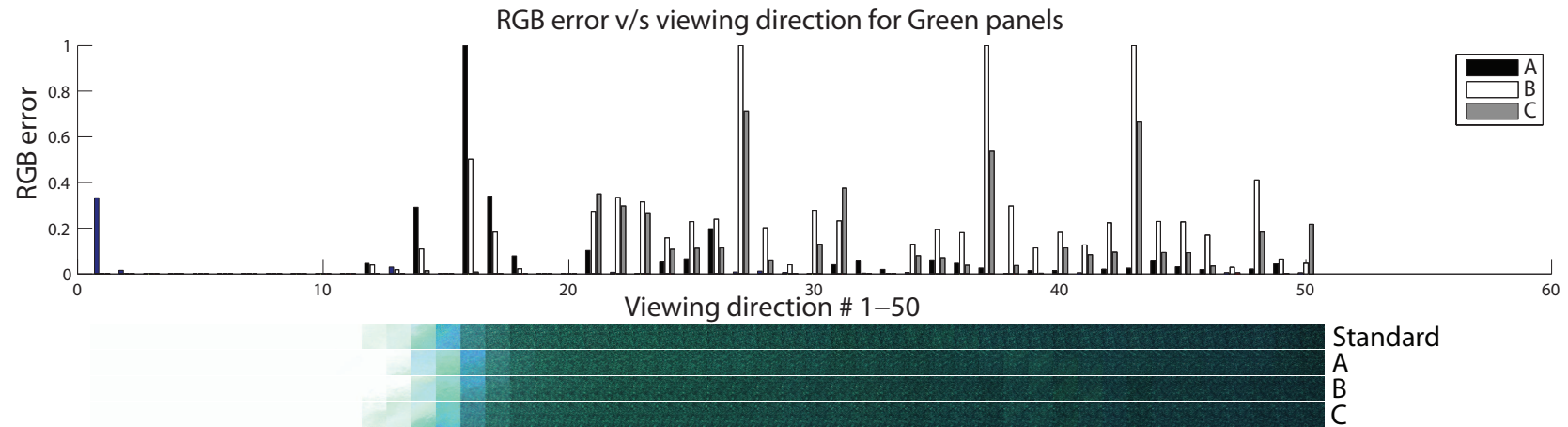
Figure 3.16: RGB error versus viewing direction for a set of OEM blue panels. Panels A, B and C are the acceptable, borderline and unacceptable match as ranked by the color matching experts. An error for viewing directions 12 through 17 indicates that the panel shows a different color travel while an error for viewing directions 20 through 50 indicates a difference in the flop color of the panel as compared to the standard. C is clearly the unacceptable match, since it has a different flop color as compared to the standard, indicated by error peaks for almost all viewing directions. B shows an error for viewing directions 12 through 17, indicating that it has a slightly different color travel as the standard, but the same flop color. It is therefore a borderline match. Panel A however, considered an acceptable match by visual judgement, shows a significant error when compared to the standard. This can be explained by observing the spatial reconstruction of the standard and panel A and noticing that the flop of the two panels is the same, the flop color of A is lighter than the standard. This causes the greater RGB error value for panel A seen in the error plot.

3.5   Matching of appearance based features using Texton Histograms

The BTF of a metallic coating as imaged by the Texcam is able to capture the coating's appearance based characteristics such as sparkle and the surface texture of the gloss in addition to the color travel. The appearance based characteristics such as the sparkle and the surface texture of the gloss represent the texture of the coating. The appearance of this texture changes drastically with different viewing/illumination directions. Figure 3.10 shows the appearance of the same spatial region of a black metallic panel as seen from 3 different viewing directions. Recognizing a coating as belonging to a particular set based on its texture in addition to the color travel based method already introduced can provide a more complete matching technique that accounts for the brightness change as well as the sparkle and orange peel.

The problem of classifying a coating as belonging to a particular set is based on the appearance of its texture is solved in the following way: given the BTF image select the surface texture (gloss/orange peel) and the subsurface texture (sparkle) and classify them as belonging to a set of pre-learnt classes. Leung and Malik [18] established the basic framework for this problem using texton histograms to describe the appearance of a surface and the chi squared distance metric to differentiate between two histograms. The texton histogram approach consists of a primitive or texton and the distribution of this texton over the image (texton histogram). The texton used for in our matching method is obtained as follows. We start by taking the set of surface and subsurface textures (sparkle and orange peel) and divide them into local nxn pixel neighborhoods. Varma and Zisserman in [19] demonstrated that superior classification results can be obtained by using compact, local neighborhoods and without the use of filter banks. We then cluster the output. The motivation for the clustering is that the finite number of local structures such as the bumps on the orange peel and the distribution of the flakes in the sparkle will form clusters. The clustering of the neighborhoods are the textons. The local structures are given a texton label and the texton histogram of the image is then computed.

Within each texture image there are generic structures such as the bumps and pits
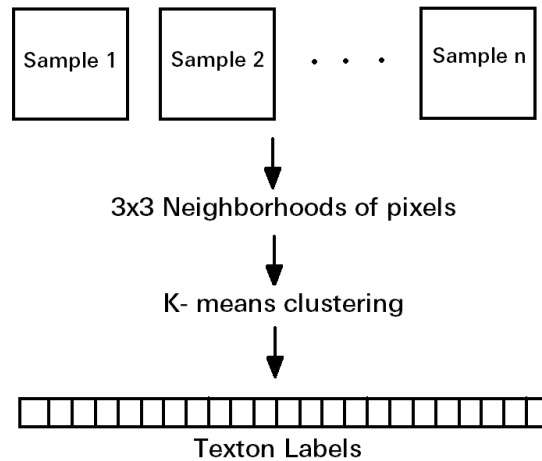
Figure 3.17: Creation of the image texton library. The set of texture images from the BTF of each of the paint samples are first divided into neighborhoods of 3×3 pixels. These neighborhoods form vectors in the feature space. The feature space is clustered using k-means to determine the texton labels for the features.

of the orange peel and the distribution of flakes in the sparkle. Figure3.17 illustrates the pre-processing step of constructing the image texton. We use a 3x3 window to form neighborhoods of pixels. These neighborhoods are the feature vectors on which we use K-means clustering to get the image textons. Because the number of available coatings is limited to 15 we use jackknifing i.e. we create subsets consisting of 14 samples of the coatings to create the texton library and test our method by finding a match for the 15th sample. An example of such a texton histogram for the subsurface texture of two black metallic samples belonging to different sets is shown in Figure3.19. Notice that these histograms are very different from each other, thus allowing good discrimination. The χ^2 significance test is used to provide a measure between the similarity of two texton histograms.

Three distinct textures obtained from the multiview image were used to classify the panels. These three textures consisted of 2 different views of the sparkle and one view of the orange peel of the coating i.e. the surface texture of the gloss as shown in Figure3.18. Since the texture images were of size 50×50 pixels, a 3×3 window was used to convert the image to a feature vector of size 9×272. K means clustering with k=15 was then used to cluster the feature vector. The clusters or textons were then
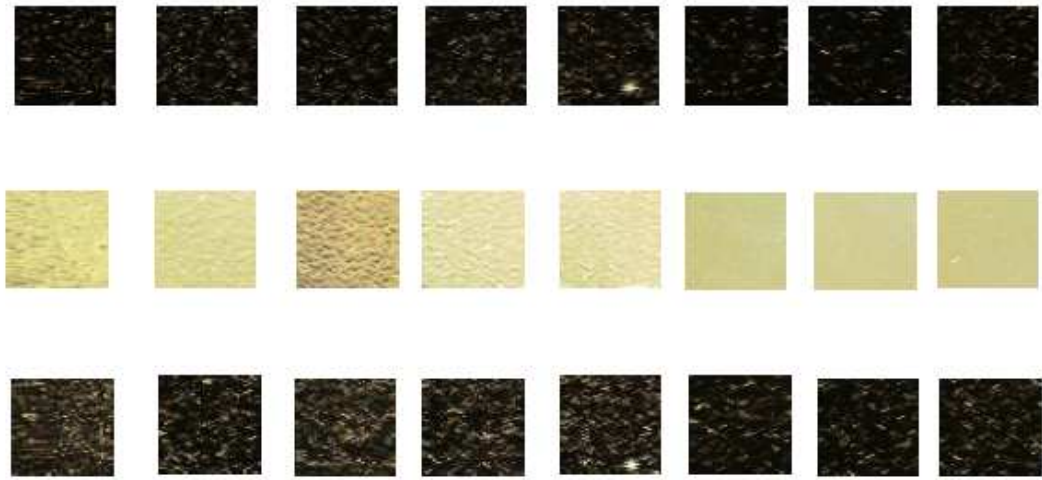
Figure 3.18: Textures used to classify the black metallic paint panels.Three distinct textures obtained from the multiview image were used to classify the panels. These three textures consisted of 2 different views of the sparkle and one view of the orange peel of the coating i.e. the surface texture of the gloss.

given labels from a precomputed texton library. The texton histogram was then used to describe the appearance of the texture. The χ^2 distance was used to compare the texton histograms and determine whether the panel in question belonged to set A, B or C, Since only 15 panels were available, jack knifing was used for validation of the method. Out of the 15 panels, 13 were correctly classified. The misclassified panels were B1 and C1. This misclassification may be explained by observing the BTF of the two panels shown in Figure X and noting that they have the same color travel. Further, their surface and subsurface textures i.e. their sparkle and gloss are similar in appearance as seen in Figure3.20. Thus the texton histogram approach can successfully classify the panels as belonging to a particular sets based on the appearance of their sparkle and orange peel. We can combine the texton histogram approach for matching the appearance based characteristics such as the sparkle and orange peel with BRDF based matching method to develop a matching technique that takes into account all the important visual attributes of the metallic coating and shows a high correlation with the visual judgement of the color matching experts.
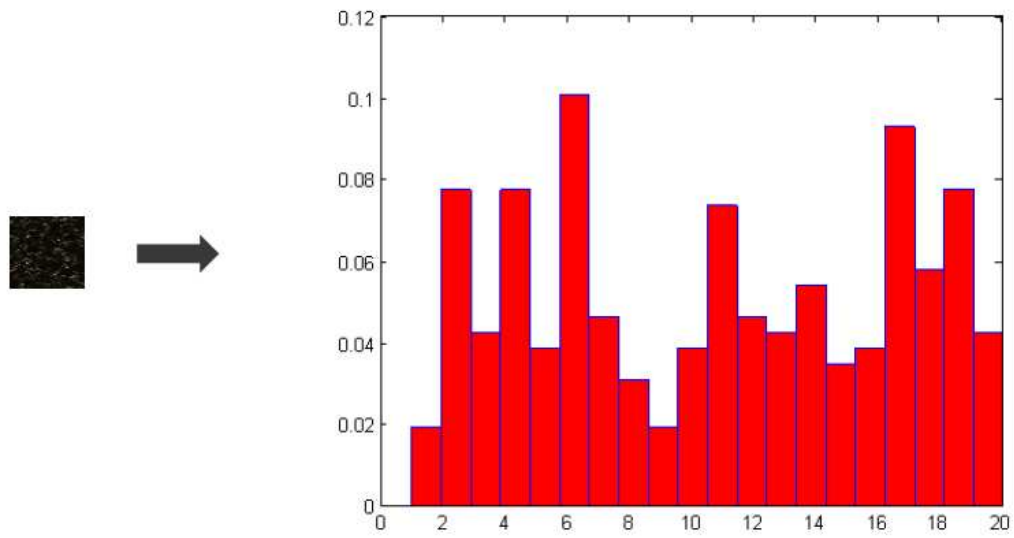
Figure 3.19: Texture representation of the sparkle using the texton histogram. The texture image of the sparkle of a black metallic coating is divided into neighborhoods of 3×3 pixels to form feature vectors. The feature vectors are projected onto the space spanned by the elements of the image texton library and are then labeled by determining the closest texton by projecting them onto the space spanned by the elements of the image texton library. The distributions of labels over the image are then represented the texton histogram.
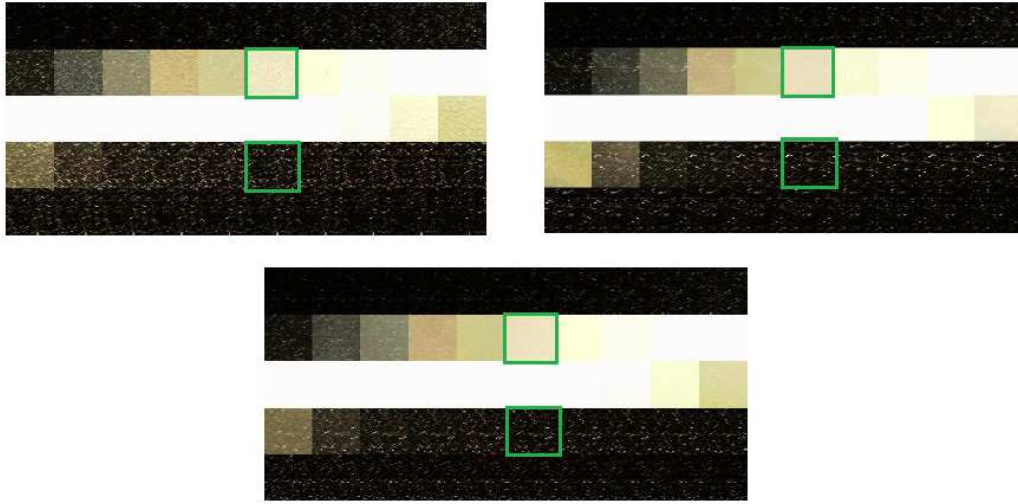
Figure 3.20: Misclassified paint samples. Panel B1(seen on the left) was classified as belonging to set C while panel C1(seen on the right) was misclassified as belonging to set B. This misclassification is due to the fact that the surface and subsurface texture i.e. the sparkle and gloss of panel B1 and those of the panels from set C(shown below) are similar in appearance.The reverse is true for panel C1, its gloss and sparkle closely match that of set B.

3.6   Discussion and Implications

A completely automated and objective matching technique for automotive coatings has been developed using the Texcam. The Texcam was used to reconstruct a 5mm×5mm patch of each of the panels as seen from 50 different viewing directions. The different views of the patch were then put together to form a composite spatial reconstruction. The precise color travel of the coating, as well as it appearance based characteristics such as the orange peel, primary specularity and sparkle due to the flakes were all observed in simultaneously in the composite spatial reconstruction. This image also makes it possible to quantify the color travel of the coating as its BRDF and match the panels based on their BRDF. In addition, the texton histogram method provides a way to match the appearance based characteristics of the coatings such as their sparkle and orange peel. These matches produced by the Texcam were shown to have a high correlation with the professional judgement of the color matching experts. Furthermore, the analysis and matching of a metallic coating by the Texcam is extremely fast -

the imaging of the surface from 50 different viewing directions and the subsequent comparison is achieved in under 15 seconds. The large number of viewing directions that can simultaneously be imaged by the Texcam makes it superior to a conventional multi angle spectrophotometer. Metallic effect pigments that contain aluminum or mica flakes as well as newer families of pigments like Xirallic exhibit an intense sparkle when viewed under direct sunlight. This sparkle can neither be captured nor sufficiently characterized with traditional multi- angle spectrophotometers [3]. Also, unlike the conventional multi- angle spectrophotometer, the color travel information obtained using the Texcam is independent of the orientation of the panel [17]. These features of the Texcam make it a potential viable solution for automated matching of metallic flake finishes.

Chapter 4

Synthesis and Rendering

Automotive as well as paint manufacturers have shown considerable interest in the accurate and photo realistic rendering of these metallic paints. Such 'virtual prototyping' will allow the customer to preview and evaluate the appearance of a particular coating either as seen on a virtual paint panel or on a computer model of the car without having to go through the time consuming and expensive process of spray painting the entire car. However, the complex appearance characteristics of the coating such as its color travel, sparkle, depth effects, orange peel etc makes the rendering of the appearance of a metallic paint a non trivial task.

The two widely used approaches to rendering car paint are analytical modeling of the paint and image based rendering. Ershov et al.[20] decompose each layer of the paint into thin imaginary sublayers, so that multiple scattering within sublayers can be ignored. A large number of parameters are used to determine the light scattering from each of the sublayers using a method known as doubling and the BRDF of the entire coating is found using a method called adding. However the texture of the sparkles are pre computed and the method does not capture the depth effect of the metallic paint. Ďurikovič explicitly modeled the geometry of the sparkles and was able to simulate the sparkling of the flakes as well as the depth effect[21]. The approach allows for the rendering of dynamic scenes with camera zoom in/zoom out. Both methods however, require user tuning of the parameters until the result looks like what is expected. This problem is overcome using image based rendering Guenther et al.[22] use a simple BRDF measurement system which includes an accurate turn table, a high-quality digital camera, a point-like LED light source, and a sphere painted with metallic paint as the acquisition target. The measured data is then fitted to a Cook - Torrance BRDF

model and used for rendering. The sparkling effect of the flakes is simulated by using a procedural texture map that holds the normals of the flakes. Instead of performing BRDF measurements and then using a sparkle simulation, Rump et al.[23] capture the whole spatially varying appearance using BTF measurements. The measurements are done using a large device consists of 151 digital consumer cameras mounted on a hemispherical gantry. The original BTF data is then split into a homogeneous part, modeled by a BRDF and a spatially varying part which is represented by the measurements minus the BRDF part and is reconstructed using image-based rendering. The setup used to capture the BTFs in this method however is large and costly to build. Instead, we make use of the Texcam and texture synthesis to produce photorealistic rendrings of the metallic coatings.

The BTF of a surface as measured by the Texcam is small, usually having dimensions just a few centimeters wide. Although small, these measurements accurately capture the appearance of the surface from multiple viewing and illumination directions. They are therefore well suited for photorealistic image based rendering of visually complex surfaces. However for practical rendering applications, the surface should be able to cover a much larger area, for instance the BTF of a metallic paint sample should be able to cover an entire virtual car. In order to cover a larger surface area using the small BTF patches, we need some way of synthesizing larger images from the small input patches. As seen in Figure4.1 a simple approach such as tiling or repetition of the patches does not provide satisfactory results. No matter how much smoothing is done across the edges of the repeated tile, the individual tiles are still conspicuous. Texture mapping in computer graphics programs such as OpenGL uses this approach and simply repeats the input texture to cover the surface to be rendered. Using the patch as an input texture to a graphics program is therefore not feasible. To overcome this we use a more sophisticated approach and make use of texture synthesis. The texture synthesis method grows a new larger image from a smaller input sample and so is well suited to BTFs. In particular we extend Efros and Freeman's image quilting algorithm[24] so that we can apply it to our measured bidirectional texture functions.
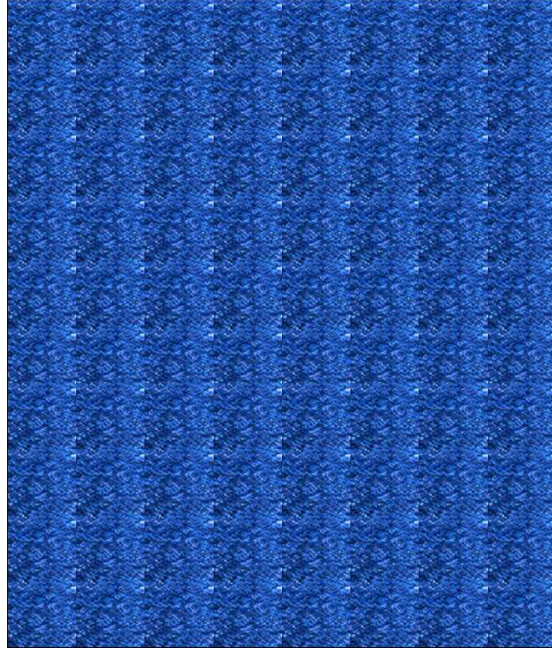
Figure 4.1: Results of tiling an input texture. A simple approach such as tiling for growing a larger image from an input texture does not provide satisfactory results. The repeated tiles are clearly visible and will remain conspicous, no matter how much smoothing is done along the edges.

4.1 Image Quilting Algorithm

Efros and Freeman [24] proposed a method for obtaining larger surface from a smaller input sample using overlapped irregularly shaped patches in their image quilting paper. They transform the overlap region between a new patch and the already synthesized texture into an error map, and then use Dijkstras algorithm[25] to find a lowest cost path through the error map between the boundaries of two adjacent patches. This is called the minimum error boundary cut, and it attempts to give the patches a ragged edge so as to minimize the error along the boundary path. In so doing, the minimum error boundary cut helps to preserve localized high-frequency structure within the input texture. This makes it a particularly useful technique for synthesizing larger images of metallic car paint whose texture shows distinct, localized features.

The quilting algorithm (as well as most traditional texture synthesis methods) has two major drawbacks when used for synthesizing textures when the input sample to it consists of multiple views of the same surface. The first drawback has to do with the fact

that the quilting algorithm is designed to work with images of a surface as seen from a single viewing and illumination direction, and results in certain spurious artifacts when the input to it is a higher dimensional texture such as a BTF. When the unmodified quilting algorithm is run on the BTF patches obtained from the Texacm that represent the different views of the same sample surface, the appearance of each of the new images is realistic. Each larger image representing a particular view, appears to be individually consistent with the original sample surface. However when the larger synthesized images are viewed as a set of different views of the same surface, the texture of each image is inconsistent with the previous view. While scrolling through the sequence of synthesized views one after another, we notice that the texture in the synthesized image, such as the flakes of the metallic paint or the weave in the fabric appear to be moving around. This movement of the texture as the view is changed is termed as *snow effect* since it resembles the snow seen in old televisions when the station is changed and the new station is not quite tuned in yet. The snow effect for multiple views of a red paint panel can be seen in Fig4.3. The quilting algorithm was intended for the synthesis of images of a surface as seen from a single viewing and illumination image and needs to be modified so that there is spatial consistency in the texture across multiple viewing and illumination directions of the same surface when the input given to it is a higher dimensional texture such as a BTF. The second major drawback is the amount of time required to synthesize a larger image for each of the viewing directions in the input multiview image. Given the large number of viewing directions imaged by the Texcam, synthesizing multiple views of a surface from a single illumination direction, the output image having a size of $512 times 512$ pixels can take several hours. The time required to synthesize multiple views for multiple illumination directions is impractical.

Both these problems can easily be solved with a simple yet effective modification to the texture synthesis algorithm. We introduce sequential numbering of the pixels to achieve spatial consistency in the multiple views of the output texture and remove the snow effect. In this approach, a patch corresponding to a viewing direction that has significant amount of detail is chosen. This may be termed as the master patch and its pixels are numbered sequentially in raster scan order. The pixels of all other

patches must have the same numbering, since they are different views of the same spatial region of the sample surface. These pixel labels are then stored as the fourth dimension of the patch (the first three dimensions being the R, G and B values of the pixels).The quilting algorithm is then applied to this 4D image and a larger image of the master patch, the master panel is synthesized. The remaining views of this master panel can now be synthesized without applying the quilting algorithm. To synthesize a different view of the panel, the labeled pixels from the desired view are simply copied and arranged according to the sequence of labels in the master panel. Because the quilting algorithm is run only once to synthesize the master panel, this modification introduces the added advantage of a drastic reduction in the time required to synthesize the remaining multiple views of the panel. The steps involved in this modified quilting algorithm are illustrated in Fig4.2. The synthesized multiview images are shown in Fig4.3
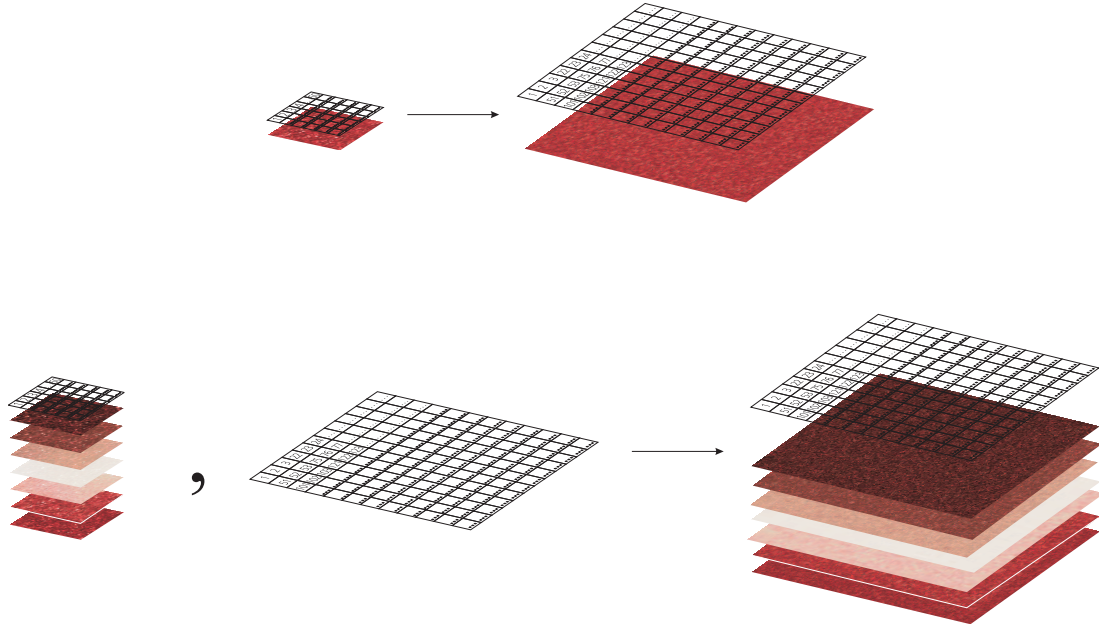

Figure 4.2: The modified quilting algorithm. Top: Each pixel of the patch is numbered sequentially and the quilting algorithm is used to synthesize a larger image. The numbering of the pixels is used to record the placement of the pixels in the output image. A template is thus obtained. Bottom: Synthesis of multiple views of the patch. The pixels from the input view is compared to the template and the pixels are places into the template according to their numbers. This simple modification introduces spatial consistency between different views for the output texture and removes the snow effect.
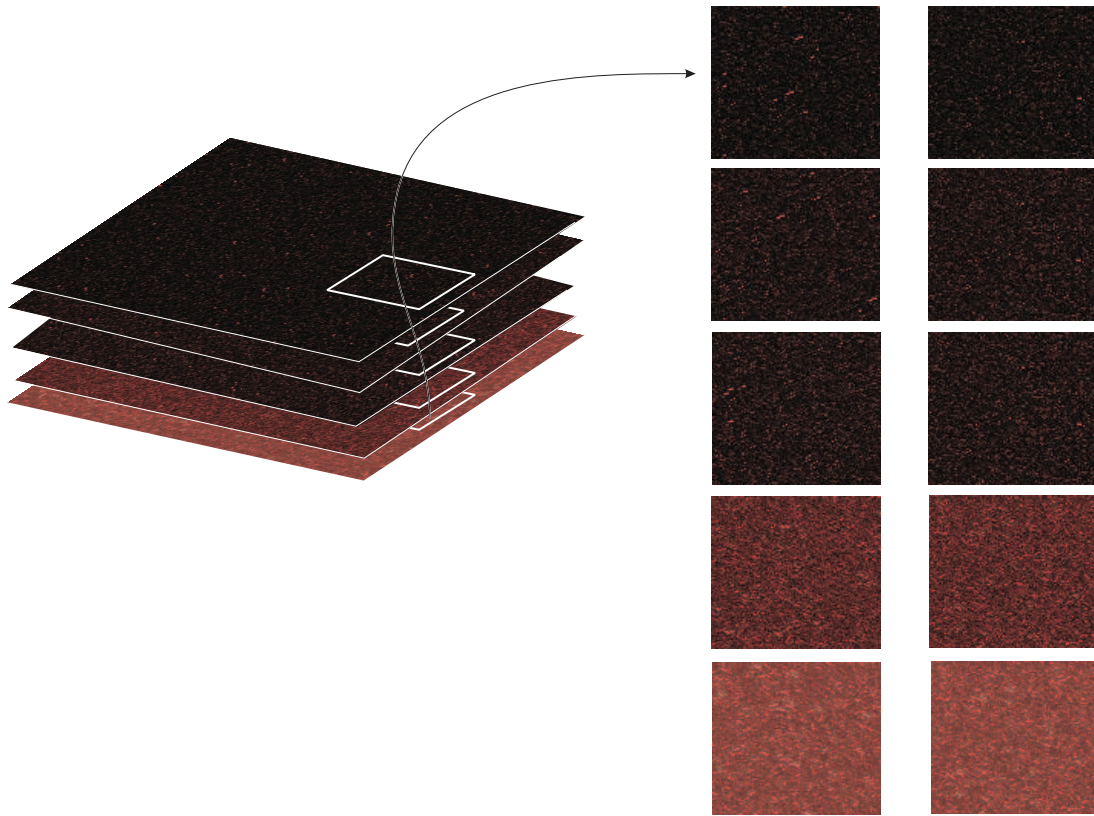
Figure 4.3: Spatial consistency in synthesized textures for multiple views. Shown in the figure is a close up of a section of the synthesized textures for five different views of the same spatial region. Notice how in the results of the unmodified synthesis algorithm, the texture (i.e. the distribution of the flakes or the sparkle) seem to move around or randomly appear in subsequent images. On the right are the results of the modified algorithm. The texture shows spatial consistency - the distribution of the flakes remains the same, but its reflectance changes
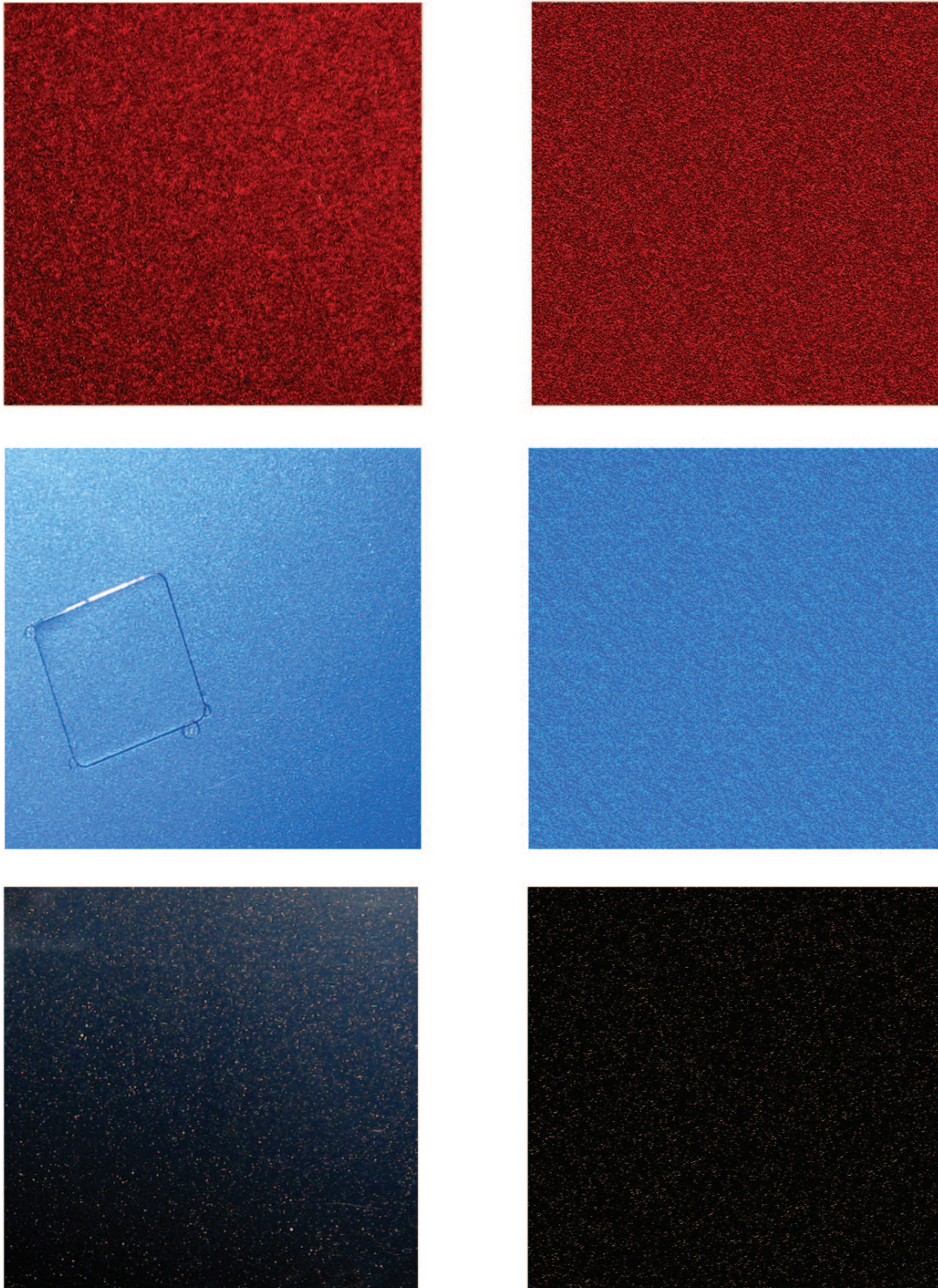
Figure 4.4: Real and Rendered Paint Panels. The Texcam was used to measure the BTF of three metallic coatings - black, blue and red. Photographs of the coatings taken in bright sunlight are seen in the top row. Shown below them are the images synthesized from the BTF of the panels as measured by the Texcam. Notice the realism of the rendering. All the important visual effects of the coating such as the color, sparkle, depth effect and distribution of flakes have been photorealistically reproduced in the rendered version

4.2   Discussion and Implications

The Texcam is able to capture the appearance of the metallic coatings over a continuum of viewing and illumination angles. The BTF of the coatings as imaged by the Texcam captures all the significant appearance based characteristics of the coating such as the color travel, gloss, sparkle and orange peel. A novel texture synthesis algorithm is then used to grow larger images from the BTFs. The modified quilting algorithm has the capability of handling multi dimensional input textures such as BTFs, besides ensuring that the synthesized images show consistency in the spatial distribution of their texture. Sequential numbering of the pixels in the input texture removes the snow effect as well as reduces the time required to synthesize multiple views of the same surface. The synthesized textures can then be mapped onto a virtual surface such as a paint panel in OpenGL to produce a photorealistic rendering of the original coating that shows all its visually important characteristics. Such virtual paint panels can be used to communicate information about the appearance of a sample to a customer or remote user without physically sending him the sample. It can also be used to cover the surface of a virtual 3D model of a car. Such virtual prototyping will allow the customer to preview and evaluate the appearance of a particular coating either as seen on a virtual paint panel or on a computer model of the car without having to go through the time consuming and expensive process of spray painting the entire car.
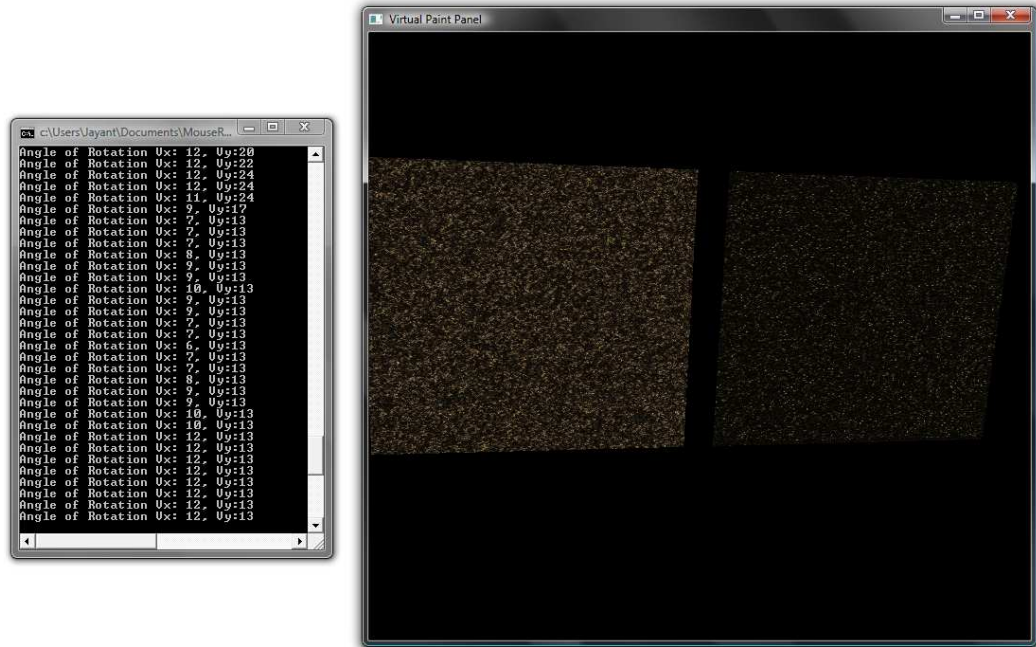
Figure 4.5: Rendering of a Black Paint Panel. The images synthesized using the input from the Texcam and the modified quilting algorithm are texture mapped onto a virtual paint panel in OpenGL. The interface allows the user to view the appearance of the coating from any desired angle, as well as rotate, zoom and translate the panels. Two or more panels can also be viewed simultaneously to compare their appearance. Notice the detailed appearance of the sparkle in the rendering. The virtual panel displays the same sparkle, color travel, surface texture (orange peel) as the original coating. Such a virtual sample can be used to communicate the appearance of any finish to a customer or remote user.

Chapter 5

Beyond Metallic Coatings: Material Recognition using the Texcam

Human observers are very good at determining the material of an object from its visual appearance. The visual appearance of a surface depends on its relfectance properties as well as the viewing and illumination geometry. The reflectance of a surface can be characterized by its BRDF. In section 3 we saw how the Texcam is able to measure the reflectance of a surface and capture its BRDF over a partial hemisphere of viewing angles. We will now exploit the BRDF images from the Texcam to develop a material recognition scheme that focusses on recognizing a material from its measured reflectance.

Material recognition is a challenge that is of considerable importance in computer vision. Unlike object recognition techniques which depends on shape and structure[26][27], material recognition is dependent on the reflectance of a surface. Besides the color, the texture and reflectance of a surface also provides us with cues about the characteristic features of a particular material e.g. is the surface rough or smooth, glossy or matte. A method for identifying the higher level material category from photographs by combining color, texute and reflectance features using an augmented Latent Dirichlet Allocation framework was presented in [28]. Another method of material recognition is to classify a material is to use texture features as presented in . However material recognition using the BRDF of a surface has received little attention. The major hurdle in using the BRDF of a surface for material recognition has been the inability to capture the BRDF over a continuum of viewing and illumination directions. The Texcam allows us to conveniently capture the BRDF of a surface over a partial hemisphere of viewing angles. This BRDF image of a surface as seen by the Texcam provides

information about its color, texture and change in appearance with viewing and illumination geometry. The Texcam image is therefore well suited for the problem of material recognition.

5.1   Material Database

In order to evaluate the capability of the Texcam in recognizing materials we have used 9 common real world materials. The materials include metallic paint, leather, stone, wood, a CD, a peacock feather, velvet and silk. 10 Texcam images of different spatial regions of the material are captured. Of these 90 images, Besides being commonly encountered, these materials show a broad variety of visual effects, ranging from texture such as gloss, silky and matte finishes to variation in color and brightness. 45 are used for training and the remaining 45 are used to evaluate the performance of the material recognition technique. A sample of the images from the database are shown in Figure5.2. As seen in the figure, the Texcam images are unique for each material and can easily be used to classify them as belonging to a particular type of material class.
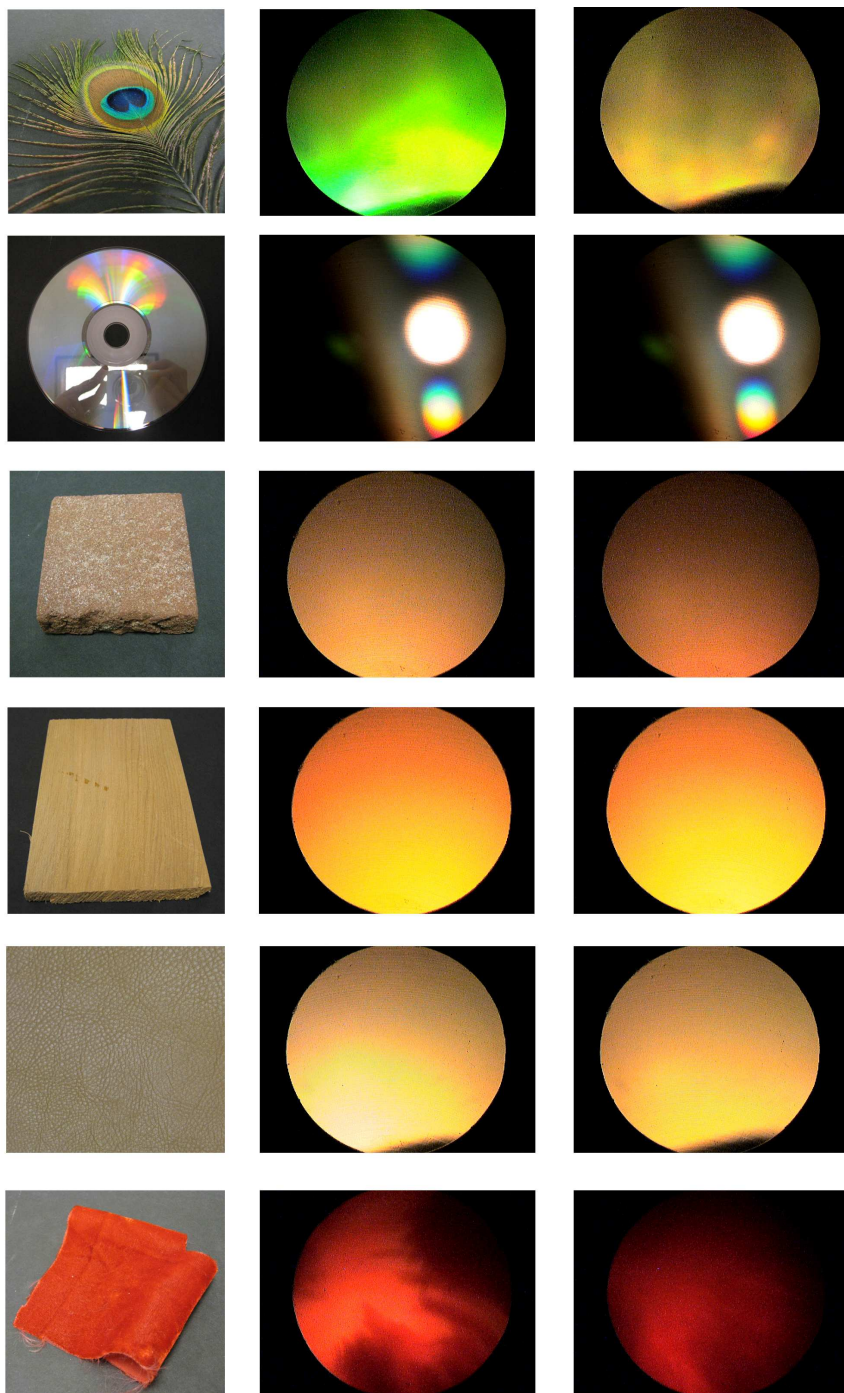
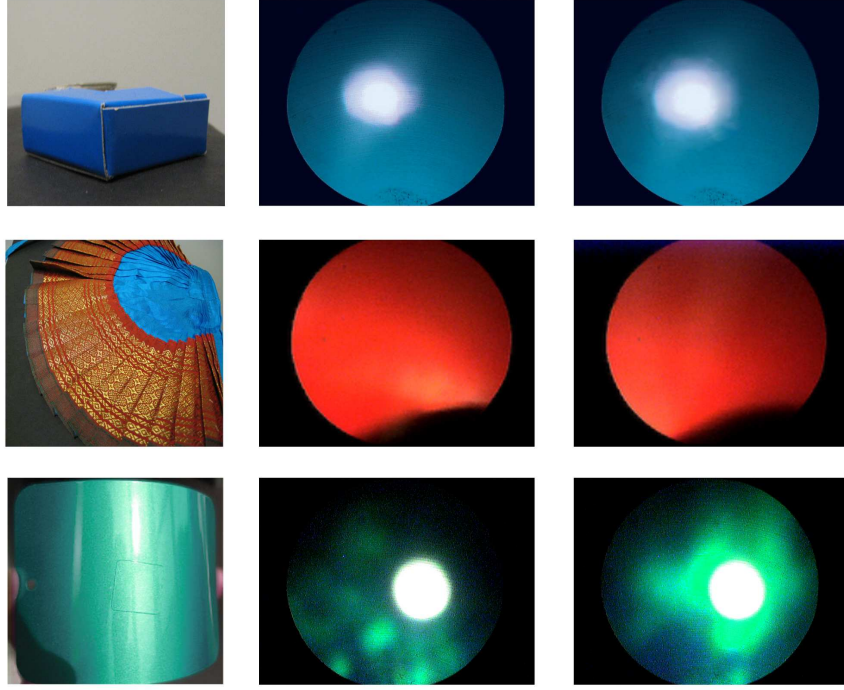Figure 5.1: Materials used in the database and their Texcam images

Figure 5.2: Materials used in the database and their Texcam images. The materials database consists of 9 commonly encountered materials: a peacock feather, a CD, stone, wood, leather, velvet, blue glossy card, emroidered silk and metallic paint. Seen to the left of each material are its corresponding Texcam images. Notice how the reflectance of each material gives rise to a unique Texcam image, which forms the basis of our material recognition technique.

5.2   Recognition Method

The material recognition problem being tackled is as follows: given a Texcam image consisting of multiple views of a surface point under a single illumination direction, categorize it as belonging to a set of pre- learnt material classes. To classify the Texcam image, we will treat the measured reflectance seen in the image as a texture and use a texton histogram approach to characterize it. Leung and Malik [18] established the basic framework for this problem using texton histograms to describe the appearance of a surface and the chi squared distance metric to differentiate between two histograms. The texton histogram approach consists of a primitive or texton and the distribution of this texton over the image (texton histogram). The texton used for in our matching

method is obtained as follows. We start by taking a random set of training images of a surface as imaged by the Texcam and divide them into local n×n pixel neighborhoods. Varma and Zisserman in [19] demonstrated that superior classification results can be obtained by using compact, local neighborhoods and without the use of filter banks. We then cluster the output. The motivation for the clustering is that the finite number of local structures in the image will form clusters. The clustering of the neighborhoods are the textons. The local structures are given a texton label and the texton histogram of the image is then computed.

Within each Texcam image there are generic structures such as the primary and secondary peaks from the specularity, a change in brightness with viewing angle and edges. Figure3.17 in section illustrates the pre-processing step of constructing the image texton. We use a 7×7 window to form neighborhoods of pixels. These neighborhoods are the feature vectors on which we use K-means clustering to get the image textons. We then create the texton library from the set of 45 training images. To test our method we obtain texton histograms for the remaining 45 test images in the dataset and find the closest match for them from the texton library. The χ^2 significance test is used to provide a measure between the similarity of two texton histograms.

5.3   Experimental Results

We used our material database to evaluate the performance of the material recognition technique. There are nine material categories in the database: wood, stone, leather, silk, a CD, metallic paint, a peacock feather and velvet. Each category contains 10 images, 5 of which are used for training and the other 5 for testing the classifier. We first find the texton labels by randomly choosing neighborhoods of 7x7 pixels as feature vectors from random images in the training set. After creating the texton labels, we use a 77 window and K- means clustering to find the texton histogram of each image in the training set. These histograms form the texton histogram library. After developing the texton histogram library we find the texton histograms for each image in the testing set and classify it as belonging to a particular material category by finding the closest match for it in the texton library. 46 out of the 50 test images were correctly classified,

leading to a recognition rate of 92%. The confusion matrix shown in Figure5.3 tells us how often each category is misclassified as another. The misclassified images mainly consisted of leather being misclassified as stone. This misclassification is not surprising considering the similarity in the appearance of their BRDFs as shown in Figure5.4.

	CD	Leather	Metallic Paint	Peacock Feather	Stone	Velvet	Wood	Silk	Blue Glossy Card
CD	1	0	0	0	0	0	0	0	0
Leather	0	0.2	0	0.2	0.6	0	0	0	0
Metallic Paint	0	0	1	0	0	0	0	0	0
Peacock Feather	0	0	0	1	0	0	0	0	0
Stone	0	0	0	0	1	0	0	0	0
Velvet	0	0	0	0	0	1	0	0	0
Wood	0	0	0	0	0	0	1	0	0
Silk	0	0	0	0	0	0	0	1	0
Blue Glossy Card	0	0	0	0	0	0	0	0	1

Figure 5.3: Normalized confusion matrix for the materials database. The rows of the table represent the predicted material class using our material recognition technique while the columns represent the actual instances of the materials. 92% of the samples are correctly classified. Only the leather sample is misclassified as stone in two instances, while it is classified as being a peacock feather in one instance. This misclassification can be explained based on the similarity in the BRDFs of the stone and the brown spatial region of the peacock feather when compared to the leather.
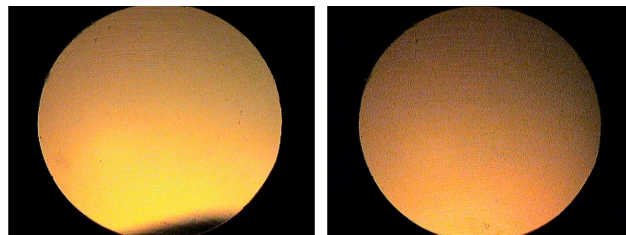

Figure 5.4: Misclassified materials. The wrongly classified materials were mostly leather which was misclassified as stone. This misclassification is not surprising considering the similarity of the Texcam images as seen in the figure.

Appendix A

Appendix

A.1 Alignment of the Texcam

The Texcam is composed of a number of components such as an illumination source, an aperture, beam splitter, parabolic mirror, a camera and a scanning stage. that are coupled together. The alignment of these components with respect to each other must be prescise so that the image captured by the camera is of the highest quality. The shape of these components and the fact that they need to be either parallel or orthogonal to each other while not necessarily lying in the same plane can make their alignment a complicated and time consuming process. Conventional instruments such as square rules are of little help when the surfaces to be aligned lie in different planes. Taking advantage of standard LEGO bricks, we will now present a quick, simple and effective method to align all the compnents with a high degree of precision.

A.2 LEGO Alignment Structures: Bases and Towers

LEGO is a higly modular construction system in which bricks of several sizes can be easily connected and taken apart by means of a patented stud-and-tube coupling. The bricks are molded in ABS(acrylonitrile butadiene styrene) and the geometric tolerances applied in the production process are quite tight, usually no more than two hundreths of a millimeter from the nominal shape and size [29]. The bricks also come in a variety of colors, so that a color that is in contrast to the Texcam components can be chosen to build the alignment structures. This contrast in color helps the user to examine the alignment of a component when the contrasting brick is held against it.

The structures used to align the compnents of the Texcam consist of a base and a

tower. The base is made up of longer bricks so that it sits on the optical bench. It is essential for alignment purposes that one end of the base falls below the surface of the bench and aligns itself with the side of the optical bench. This type of design allows the base to slide along the optical bench until it reaches its desired position as well as ensuring that one optical bench is always used as a reference for the alignment. An example of such a base is shown in FigureA.1.A tower is built on the base using shorter bricks, with the topmost bricks of the tower being yellow or color that contrasts the component that needs to be aligned. The contrasting color helps in visual examination of the alignment. The tower is fixed atop the base in various positions so that the bricks at its top touches one side of the component to be aligned. Two configurations of such a tower are shown in FigureA.2. It is recommended that a number of interlocking bricks be used to increase the stability of the alignment structure. To check that the base and tower are stable pick the structure up and shake the structure. A portion of the structure breaking off or a creaky noise from the bricks indicate that either the structure is composed of too few layers of interlocking bricks, or that the bricks have not been pressed together tightly. Once a tight and stable tower has been built we can proceed with the alignment of the Texcam. We shall now guide you through each of the steps required to align all the components of the Texcam.
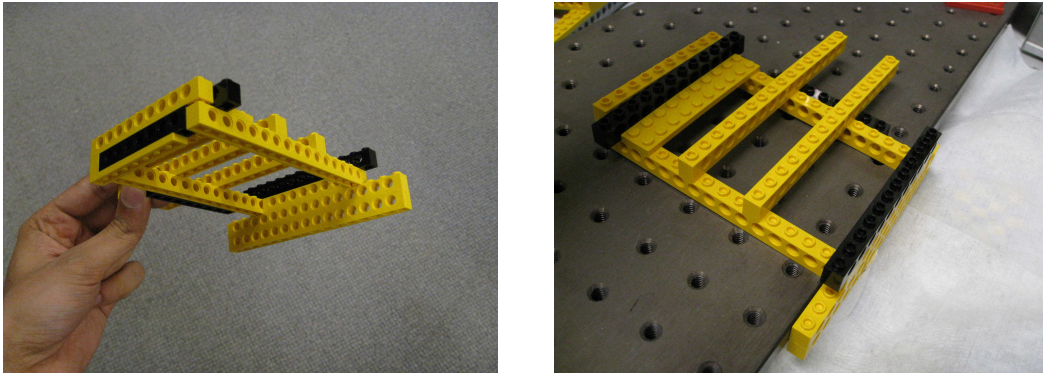
Figure A.1: LEGO Bases. The base is made up of longer bricks so that it sits on the optical bench. It is essential for alignment purposes that one end of the base falls below the surface of the bench and aligns itself with the side of the optical bench. This type of design allows the base to slide along the optical bench until it reaches its desired position as well as ensuring that one optical bench is always used as a reference for the alignment as seen in the figure.
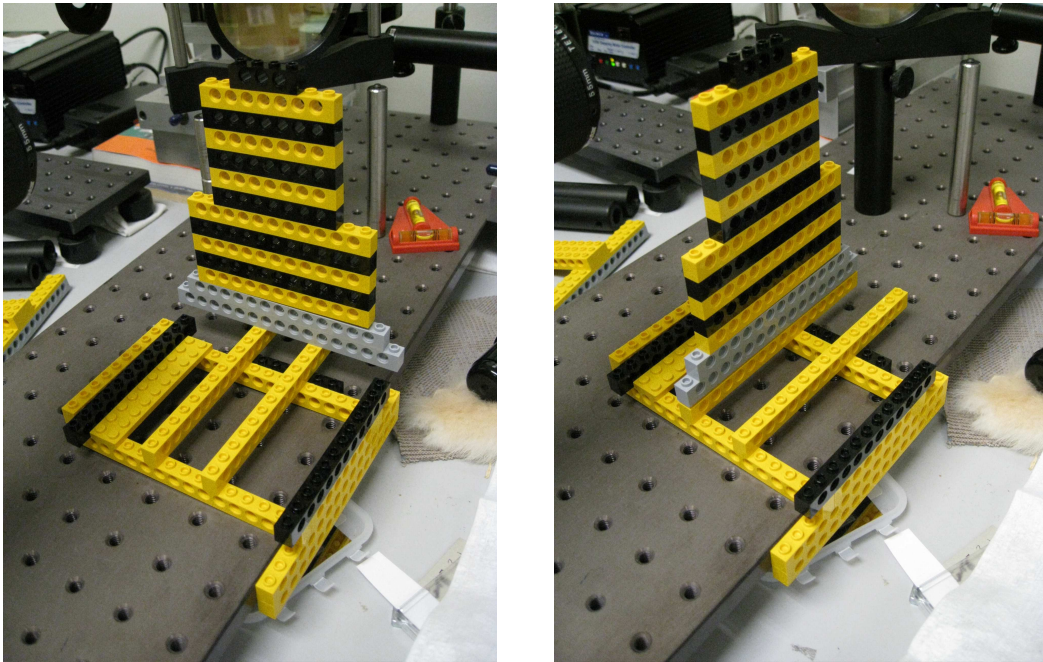

Figure A.2: LEGO towers. A tower is built on the base using shorter bricks, with the topmost bricks of the tower being yellow or color that contrasts the component that needs to be aligned. The contrasting color helps in visual examination of the alignment. The tower is fixed atop the base in various positions so that the bricks at its top touches one side of the component to be aligned.
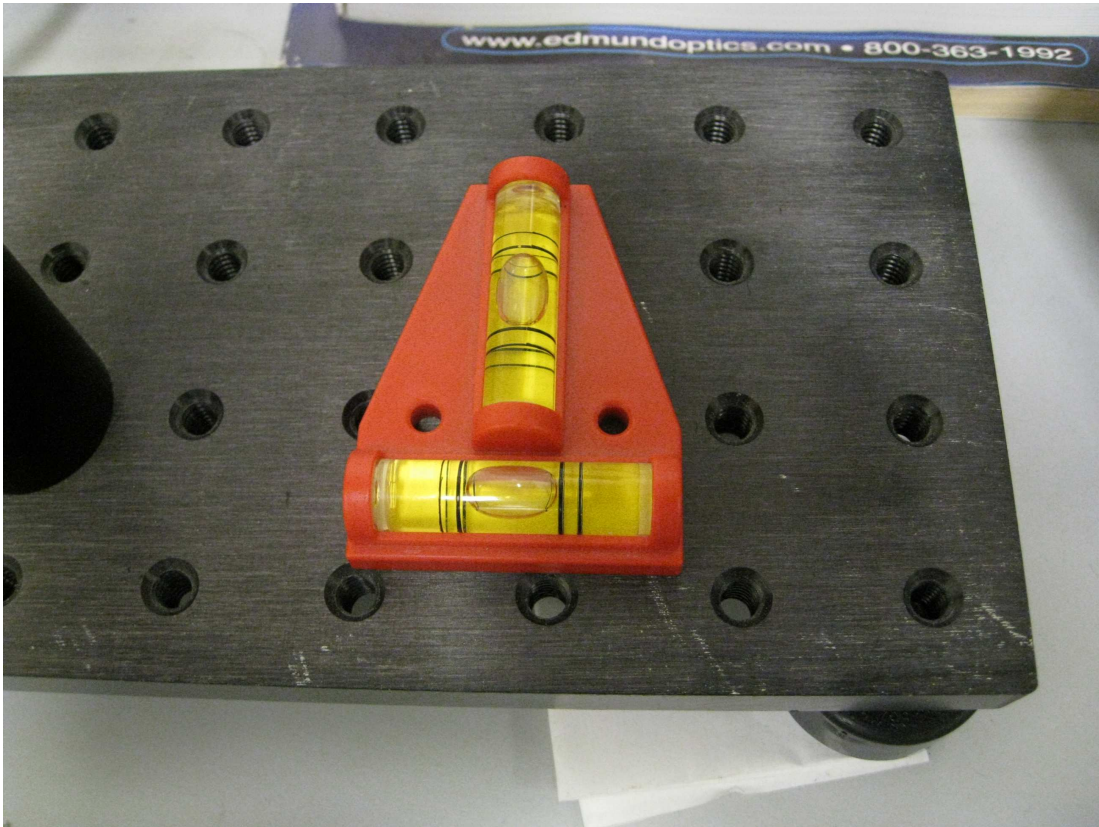
Step 1 - Level the optical benches

Figure A.3: Place the spirit level on the optical bench and turn the necessary adjustment screws at the base of the bench until both the bubbles in the tubes settle in the center.

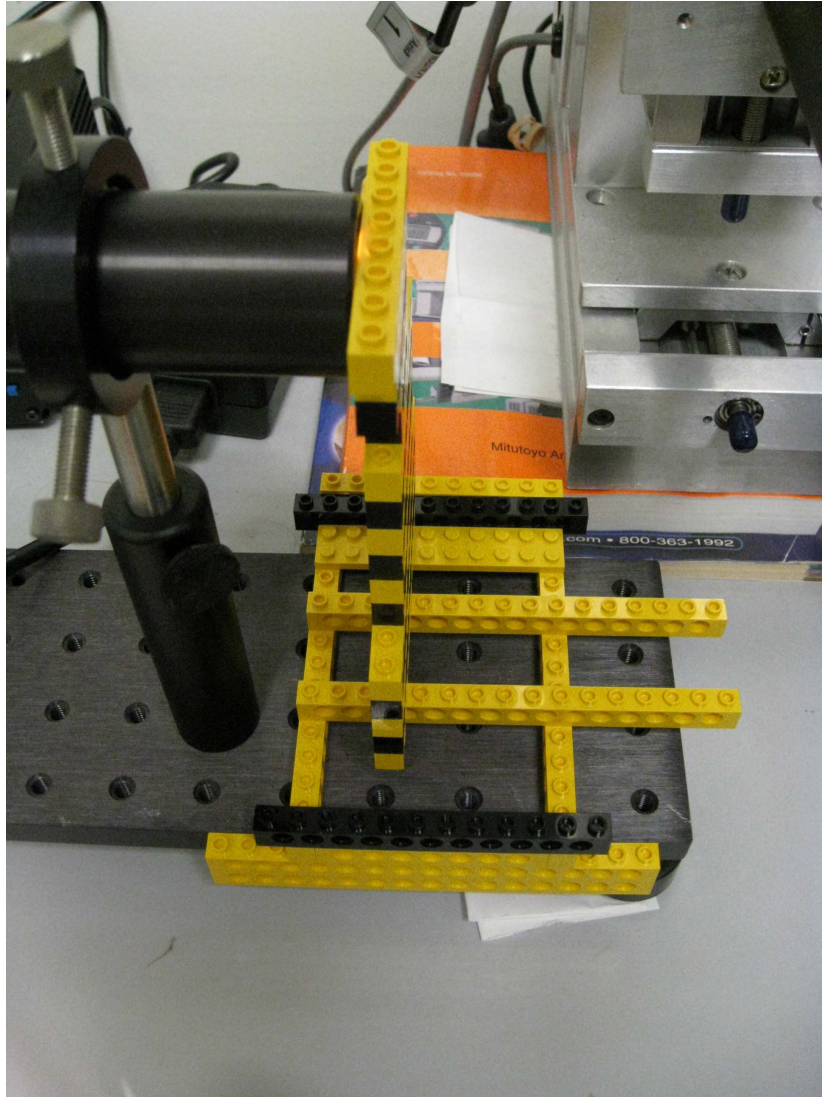Step 2 - Align the light source orthogonal to the optical bench

Figure A.4: Build a LEGO tower that touches the face of the cylinderical light source. Slide the tower along the bench until it touches the face of the cylinder. Rotate the light source about its holder until its face is perfectly touching the tower.

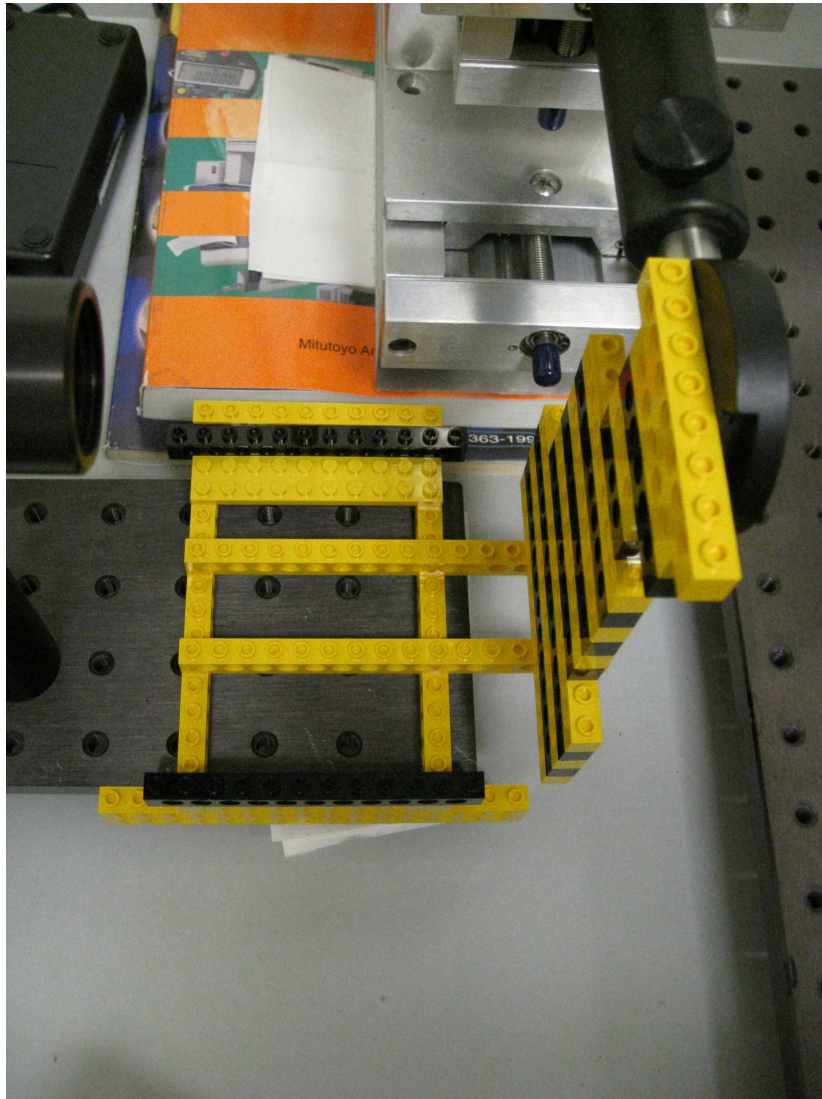Step 3 - Align the movable aperture with the light source.

Figure A.5: Now build a tower that touches the face of the movable aperture. Rotate the aperture either about its holder or since the aperture is rigidly fixed to the stepper motor, gently rotate the enitre stepper motor until the aperture is touching the tower.

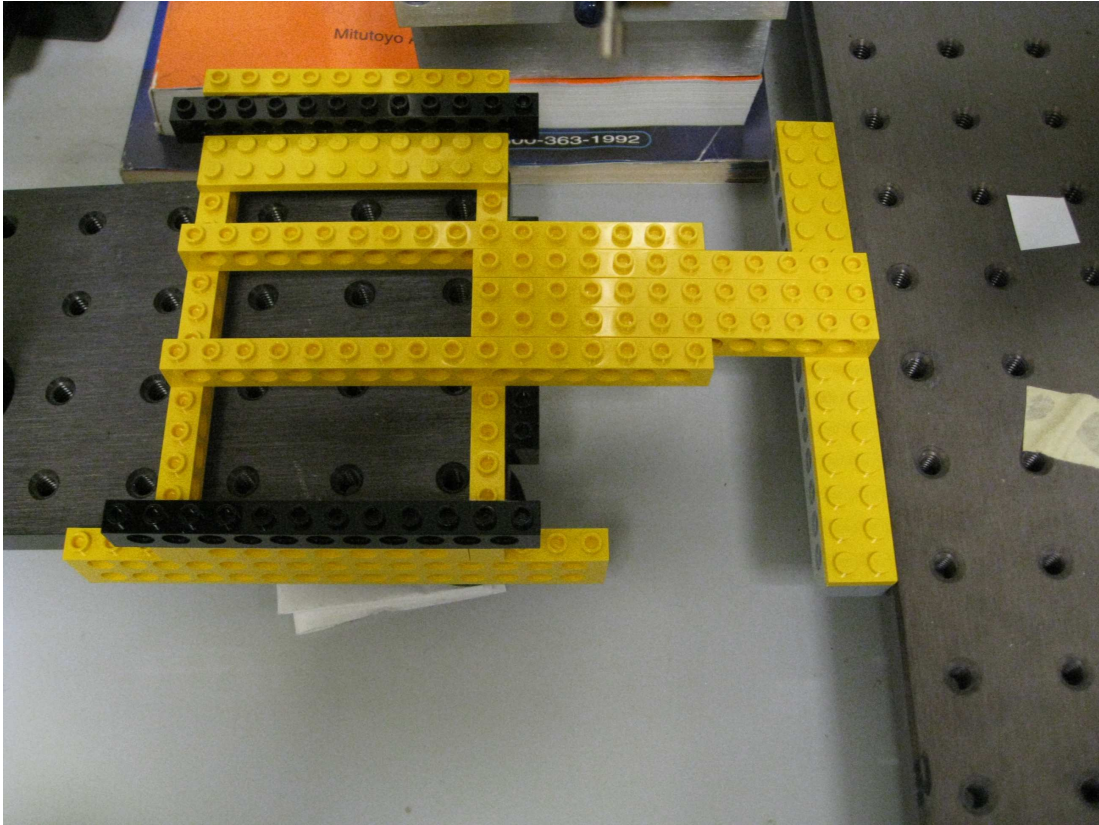Step 4 - Align the two optical benches orthogonal to each other

Figure A.6: Add more bricks to the base to extend it until it can reach the second optical bench. Such an extended base is shown in the figure. Make sure that the base is aligned with the first optical bench. Then gently rotate the second optical bench until it perfectly touches the other end of the LEGO base.

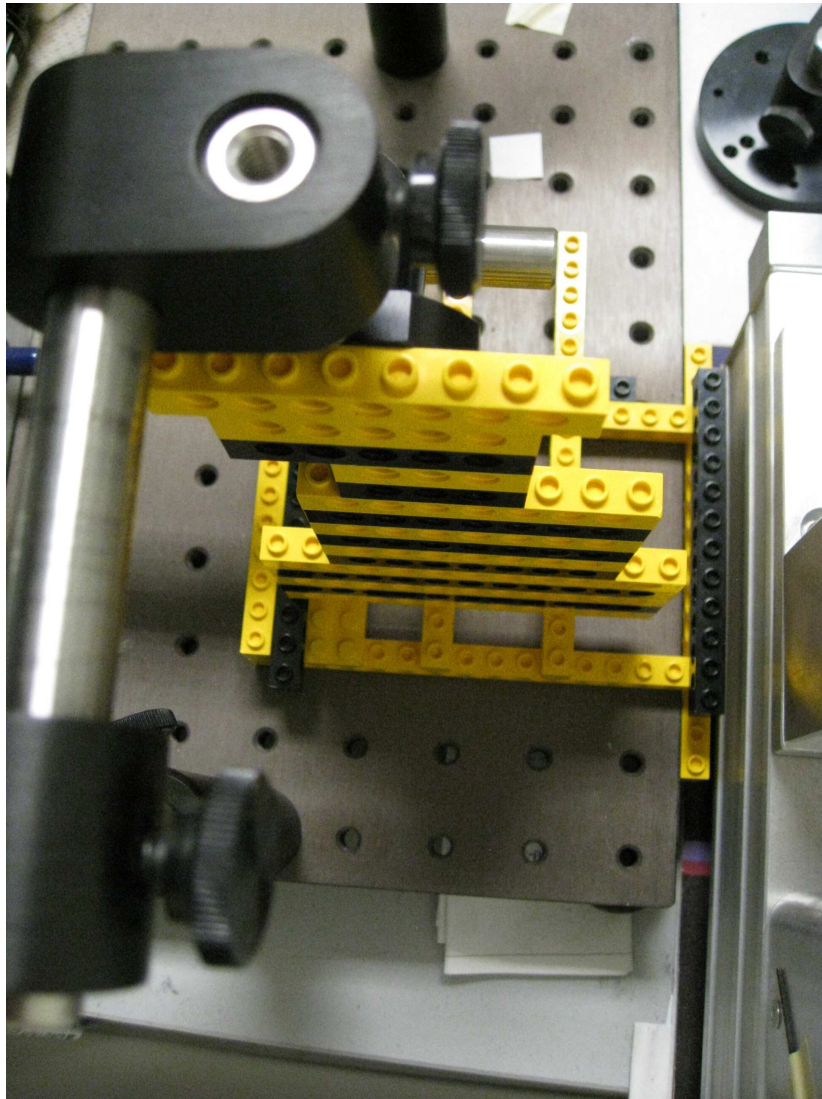Step 5 - Align the parabolic mirror orthogonal to the second optical bench

Figure A.7: Because of the special configuration of the rods holding the parabolic mirror in place, a careful design of the tower is needed. An example of such a tower is shown in the figure. Rotate the mirror about the vertical axis until it perfectly touches the tower. It is now partially aligned to the second optical bench.

Step 6 - Level the parabolic mirror

Figure A.8: To complete the alignment of the mirror, place the spirit level on the mirror mount and rotate the mount about its horizontal axis until the bubble is at the center of the tube.

Step 7 - Level the scanning stage

Figure A.9: Place the spirit level on the scanning stage and gently rotate the stage either using the mount that is fixed to it or the mount that attaches it to the stepper motor, or both until the bubble is at the center of the tube.

Step 8 - Align the beamsplitter at a 45° angle to the light source and mirror

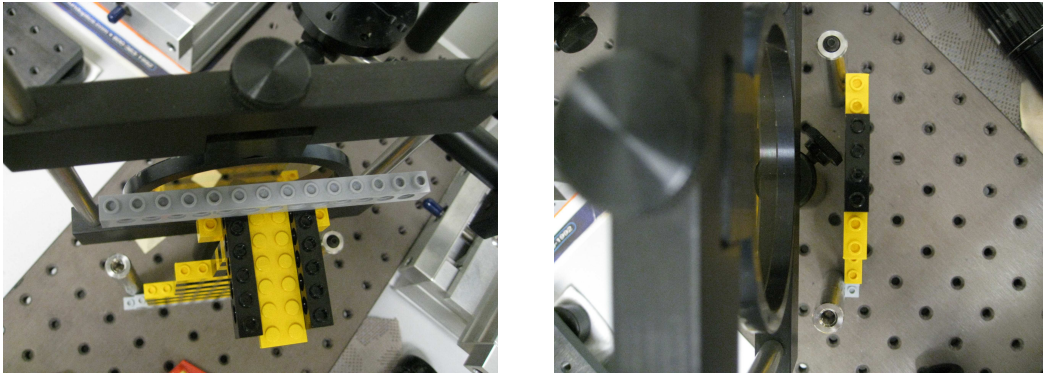Figure A.10: First screw two rods into the optical bench so that the imaginary line connecting the rods is at 45 to the edge of the optical bench. Now build a base whose edge touches both these rods. Fix a tower to this base so that the upper end of the tower touches the circular frame of the beam splitter. Rotate the beam splitter about its vertical axis until this alignment is achieved.
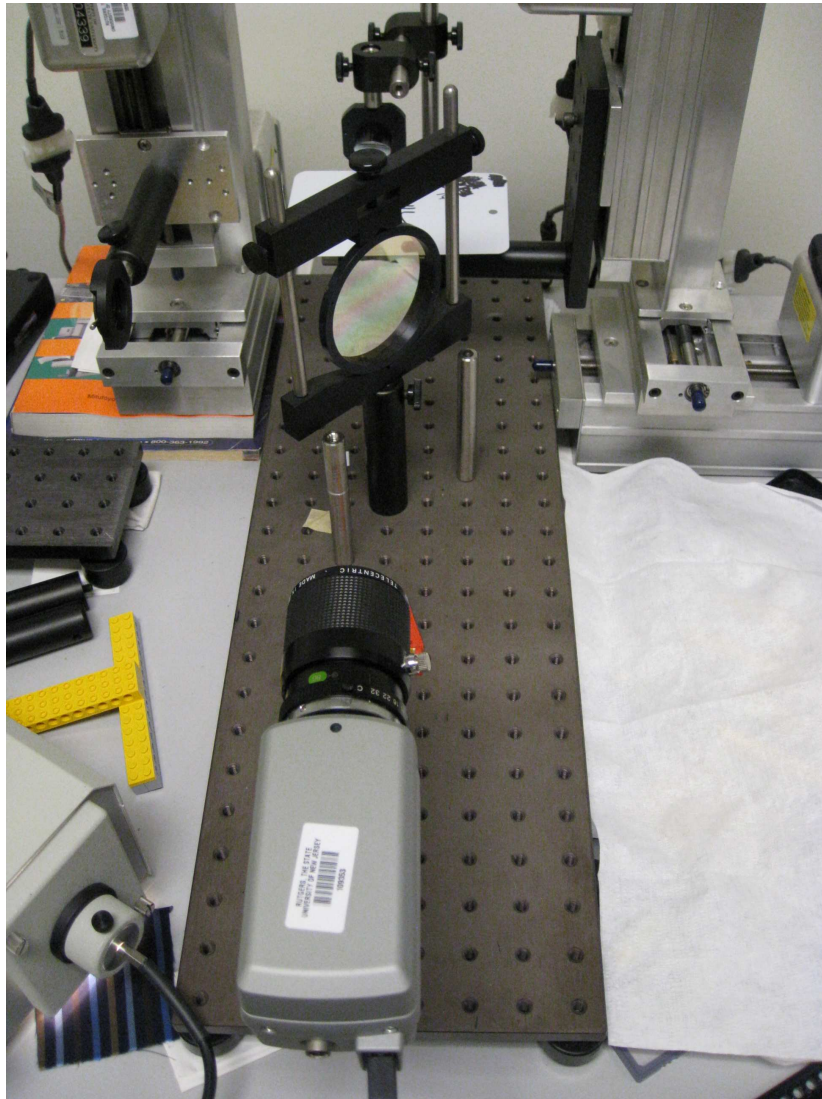
Step 9 - Align the camera to face the mirror

Figure A.11: Adjust the height of the camera using its holder and rotate it about its vertical axis until the image of the mirror on the screen perfectly fits into the circle shown in the figure.

Step 10 - Adjust the height of the scanning stage If the surface to be scanned is not at the proper height a dark yin-yang symbol like shadow will be seen within the Texcam image. After placing the surface to be scanned on the scanning stage, move the scanning stage either up or down until the dark shadows disappear. If you observe the size of the illumination spot at the scanning stage, you will notice that at the height at which the shadow disappears, the spot is in focus and is smallest and brightest as

compared to other heights of the stage.

References

[1] Robert Besold, "Metallic effect - characterization, parameter and methods for instrumental determination," *Die Farbe*, , no. 37, pp. 79–85, 1990.

[2] Gunter Buxbaum, *Industrial Inorganic Pigments*, p. 255, Wiley-VCH Verlag GmbH and Co, 1993.

[3] Jörg Schwarz Dr. Hans-Joachim Streitberger Gerhard Wagner Gabi Kiegle-Böckler, Gerhard Pausch, *Automotive Paints and Coatings*, Wiley-VCH Verlag GmbH and Co., 2008.

[4] C. S. McCamy, "Observation and measurement of the appearance of metallic materials. part i. macro appearance," *Color research and application*, , no. 21, pp. 292–304, 1996.

[5] C. S. McCamy, "Observation and measurement of the appearance of metallic materials. part ii. micro appearance," *Color research and application*, , no. 23, pp. 232–373, 1996.

[6] "Standard terminology of appearance," in *Annual Book of ASTM Standards*, vol. 06.01. 1999.

[7] Roy s. Berns, *Billmeyer and Saltzmans Principles of Color Technology*, John Wiley and Sons, Inc., New York, 2000.

[8] Larry E. Steenhoek Allan B. J. Rodrigues, "Astm e-12.12: Measurement of metallic and pearlescent colors," *Die Farbe*, vol. 42 (4/6), pp. 151–158, 1996.

[9] Gabel P.W. Cramer W.R., "Measuring special effects: A comparison of various spectrophotometers," *European Coatings Journal*, vol. 34, pp. 7–8, 2001.

[10] Fred E. Nicodemus, "Directional reflectance and emissivity of an opaque surface," *Appl. Opt.*, vol. 4, no. 7, pp. 767–773, 1965.

[11] Richmon J. C. Hsia J. J.-Ginsberg I. W. Limperis Nicodemus, F. E., "Geometric considerations and nomenclature for reflectance," *NBS Monograph 160*, Oct 1977.

[12] K.J. Dana, B. Van-Ginneken, and S.K. Nayar andJ.J. Koenderink, "Reflectance and texture of real world surfaces," *ACM Transactions on Graphics (TOG)*, vol. 18, no. 1, pp. 134, Jan 1999.

[13] Gero Müller, Jan Meseth, Mirko Sattler, Ralf Sarlette, and Reinhard Klein, "Acquisition, synthesis and rendering of bidirectional texture functions," *Eurographics 2004, State of the Art Reports*, pp. 69–94, sep 2004.

[14] K. Dana and J. Wang, "Device for convenient measurement of spatially varying bidirectional reflectance," *Journal of the Optical Society of America*, pp. 1–12, January 2004.

[15] K. Dana and J. Wang, "A novel approach for texture shape recovery," *International Conference on Computer Vision*, pp. 1374–1380, October 2003.

[16] K. Dana, "Brdf/btf measurement device," *International Conference on Computer Vision*, pp. 460–466, July 2001.

[17] D. Jeffery Davis, "An investigation of multi angle spectrophotometry for colored polypropylene compounds," *SPE/ ANTEC Proceedings*, pp. 2663–2671, 1996.

[18] Thomas Leung and Jitendra Malik, "Representing and recognizing the visual appearance of materials using three-dimensional textons," *International Journal of Computer Vision*, vol. 43, no. 1, pp. 29–44, 2001.

[19] M. Varma and A. Zisserman, "Texture classification: Are filter banks necessary?," *Proceedings of the IEEE Conference on Computer Vision and Pattern Recognition*, vol. 2, pp. 691–698, June 2003.

[20] S. Ershova, K. Kolchina, and K. Myszkowskib, "Rendering pearlescent appearance based on paint-composition modelling," *The European Association for Computer Graphics 22th Annual Conference: EUROGRAPHICS 2001*, vol. 20(3), pp. 227–238, 2001.

[21] Roman Ďurikovič and William L. Martens, "Simulation of sparkling and depth effect in paints," pp. 193–198, 2003.

[22] Johannes Günther, Tongbo Chen, Michael Goesele, Ingo Wald, and Hans-Peter Seidel, "Efficient acquisition and realistic rendering of car paint," pp. 487–494, nov 2005.

[23] Martin Rump, Gero Müller, Ralf Sarlette, Dirk Koch, and Reinhard Klein, "Photo-realistic rendering of metallic car paint from image-based measurements," *Computer Graphics Forum*, vol. 27, no. 2, apr 2008.

[24] Alexei A. Efros and William T. Freeman, "Image quilting for texture synthesis and transfer," *Proceedings of SIGGRAPH 2001*, pp. 341–346, August 2001.

[25] E. W. Dijkstra, "A note on two problems in connection with graphs," in *Numerische Mathematik*, 1959, vol. 1, pp. 269–271.

[26] Greg Mori, Serge Belongie, Jitendra Malik, and Senior Member, "Efficient shape matching using shape contexts," *IEEE Trans. Pattern Analysis and Machine Intelligence*, vol. 27, pp. 1832–1837, 2005.

[27] Serge Belongie, Jitendra Malik, and Jan Puzicha, "Shape matching and object recognition using shape contexts," *IEEE Transactions on Pattern Analysis and Machine Intelligence*, vol. 24, pp. 509–522, 2001.

[28] C. Liu, L. Sharan, E. H. Adelson, and R. Rosenholtz, "Exploring features in a bayesian framework for material recognition," *IEEE Conference on Computer Vision and Pattern Recognition (CVPR)*, 2010.

[29] http://www.lego.com/eng/info/default.asp?page=facts Retrieved July 20 2010 The LEGO Group, Company Profile: An introduction to the LEGO Group, ," .